UNIVERSITY OF CALIFORNIA, SAN DIEGO

Development of Density-Variant Glycan Microarrays

A Thesis submitted in partial satisfaction of the requirements for the degree

Master of Science

in

Chemistry

by

Bryan James Anstead

Committee in charge:

Professor Kamil Godula, Chair
Professor Seth Cohen
Professor Thomas Hermann

2017

The Thesis of Bryan James Anstead is approved, and it is acceptable in quality and form for publication on microfilm and electronically:

_____

_____

_____

Chair

University of California, San Diego

2017

Table of Contents

Abbreviations used:

Lac- Lactose

LacNAc- N-Acetyl-D-lactosamine

Glc- Glucose

GAG- Glycosaminoglycan

CRDs- Carbohydrate recognition domains

ASF- asialofetuin

MBL- Mannose-binding lectin

BSA- Bovine serum albumin

PBS- Phosphate buffered saline

HEPES- 4-(2-hydroxyethyl)-1-piperazineethanesulfonic acid

LBB- Lectin binding buffer

TAMRA- 5-Carboxytetramethylrhodamine

RCA_{120}- *Ricinus Communis Agglutinin I*

NHS- N-hydroxysuccinimide

EDTA- Ethylenediaminetetraacetic acid

TBTA- Tris(benzyltriazolylmethyl)amine

dPEG- Poly(ethyleneglycol) bisamine

EDC- 1-Ethyl-3-(3-dimethylaminopropyl)carbodiimide

THF- Tetrahydrofuran

DIPEA- N,N-Diisopropylethylamine

ELISA- Enzyme-linked immunosorbent assay

ITC- Isothermal titration calorimetry

SPR- Surface plasmon resonance

Eq.- Equivalences

List of Figures

List of Tables

Acknowledgements

I would like to thank my P.I., Dr. Kamil Godula, for providing much needed support throughout this work. I would also like to extend my thanks to Dr. Yinan Wang and Dr. Mia Huang for their advice and guidance. Furthermore, my colleague Greg Trieger helped with the polymer labeling and ligation, as well as providing support and empathy while working with the microarray printer. Additionally, I owe Sean Purcell for the glycopolymer IR data. Finally, I would like to extend my gratitude to my fellow Microarray specialist, Taryn Lucas, for being a constant soundboard and source of encouragement, as well as for allowing me to utilize her n=424 Lac glycopolymers.

I likely would not have made it this far if not for my former mentor, Dr. Tim Christensen, who incited my interest in the scientific process and pushed me towards higher education. My time in his lab was invaluable in shaping me to become a better leader, educator, and scientist. Finally, thanks is also owed to my family. To my mother, for pushing me when I needed to be pushed, and to my grandfather, for teaching me how to live life well.

ABSTRACT OF THE THESIS

Development of Density-Variant Glycan Microarrays

by

Bryan James Anstead

Master of Science in Chemistry

University of California, San Diego, 2017

Professor Kamil Godula, Chair

Glycans, and the proteins that recognize them, are involved in numerous functions throughout an organism's lifespan. Lectins, a major group of glycan-binding proteins, typically utilize multiple glycan-binding sites to fully interact with the glycans. The specific glycans preferred by lectins in a single family can be diverse, necessitating a high-throughput method of determining lectin specificity. In this study a high-throughput microarray platform consisting of glycopolymers with varying lengths and valencies, was developed to mimic natural mucins and determine how glycan valency, density, and spatial separation affect the binding and specificity of a lectin, *Ricinus Communis Agglutinin* I. A variety of surfaces were evaluated, using both "Cu-click" and "Cu-free

click" reactions to append the glycopolymers to the surface. Epoxysilane surfaces were functionalized with diaminoPEG under cloudpoint conditions, followed by coupling with propiolic acid for subsequent click reactions with the azide-terminated glycopolymers.

Then, the binding specificity of a lectin, *Ricinus Communis* agglutinin I (RCA_{120}), was assessed using lactose and LacNAc glycopolymers of varying lengths, valency, and density on the surface. RCA_{120} was determined to prefer glycopolymers printed at the second-to-highest concentration, 5 μM, as well as glycopolymers ligated with N-acetyllactosamine.

I. Introduction

Glycans

The role of glycans, which are any form of mono-, oligo, or polysaccharide, span a wide variety of functions. These include the maintenance of tissue structure, as well as mediating intrinsic and extrinsic recognition, and span from the initial development of the organism to its survival throughout life. Despite this, of the four major classes of biological macromolecules the least is known about glycans, most likely because the scientific community currently lacks the tools needed to probe their complex structures and properties.

Glycans themselves can have widely diverse structures, based on linear or branched chains of sugar residues connected by either α- or β-glycosidic linkages, as well as modification such as acetylation and sulfation.[1] Unlike proteins, glycan structures are not directly encoded in the genome. Instead, glycans are generated in an "assembly-line" mechanism of biosynthesis. This occurs in the Golgi apparatus through an assortment of competing and successively acting glycosidases and glycosyltransferases. As such, a protein encoded by a single gene can have many different "glycoforms," due to microheterogeneity, which is a term used to describe how at any glycan attachment site on a protein created by a particular cell type there can be numerous variations found in the structure of the glycan chain. Even small changes in environmental cues, such as the organism's diet, can cause changes in

glycans produced. The variable nature of glycosylation allows for vast biological diversity and complexity. However, this makes it much more difficult to parse out direct interactions and functions of glycans compared to proteins and their nucleic acid building blocks

Glycans are often found on the exterior surface of cells, in a glycoprotein-polysaccharide complex referred to as the glycocalyx. Glycans are also commonly found covalently attached to the peptide chain via N- or O-linkages of proteins, or as proteoglycans, which are heavily glycosylated proteins containing glycosaminoglycan (GAG) chains of repeating disaccharide units. The biological roles of glycans are divided into two large categories: the structural and modulatory properties of glycans, and the specific recognition of glycans by other molecules such as glycan-binding proteins.[2]

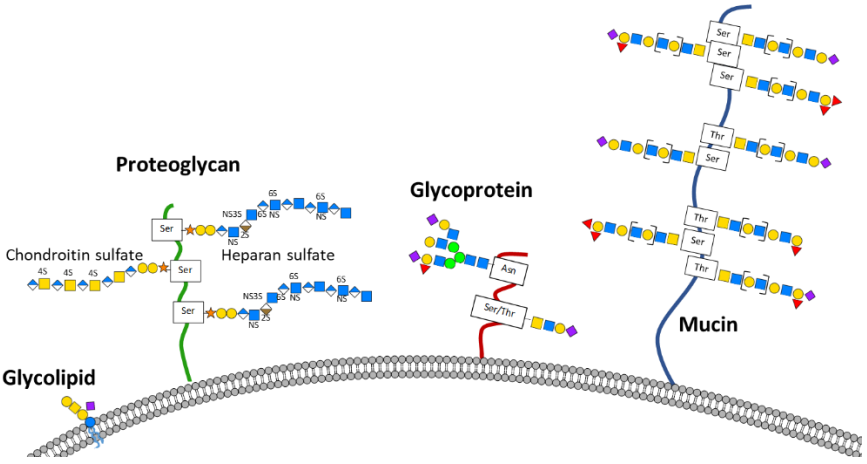

Figure 1.1: Representative cell surface glycoconjugates of the glycocalyx. There are numerous varieties that may contain different modifications, such as sulfation, phosphorylation, and acetylation. Glycoproteins are differentiated based on their underlying linkage to the peptide backbone: N-glycans are linked through asparagine residues and may be branched, while O-glycans are linked through serine or threonine. Heparan sulfate and chondroitin sulfate are typical glycosaminoglycan (GAG) chains found on proteoglycans that may vary in their sulfation patterns.

Glycan-binding Proteins

Glycans are able to facilitate their many biological roles through physical properties, but many of their more specific functions are due to their recognition by glycan-binding proteins. Glycan-binding proteins can be either intrinsic, which recognize glycans from the same organism, or extrinsic, which recognize glycans from a different organism. These glycan-binding proteins can be separated into two groups: glycosaminoglycan-binding proteins, and lectins. Glycosaminoglycan-binding proteins recognize different types of sulfated glycosaminoglycans (GAGs), and typically bind monovalently with moderate binding affinity.[3] Lectins are subdivided into C-type, P-type, I-type, galectins, and more, and these groups can be even further subdivided but are generally separated based on binding preferences. The ligand for a lectin is typically a monosaccharide residue at the terminal nonreducing end of a glycan chain, but sometimes internal sugar residues are recognized as binding partners.

The dissociation constant, K_D, is a measurement of the tendency of the ligand-protein complex to dissociate into their unbound forms, and is commonly used to describe how tightly a protein binds to a ligand. The K_D is the concentration of the ligand at which the concentration of unbound protein is equal to the concentration of the ligand-protein complex. The more readily a protein binds to a ligand, the lower the K_D. The affinity of most single glycan-protein interactions is usually low, ranging from the mM to μM K_D values.[4] However, lectins generally have multiple carbohydrate-recognition domains (CRDs), allowing them to form multivalent interactions, provided there is an optimal density of ligands to bind. The interaction of multiple lectin subunits with a

multivalent display of glycan ligand raises the affinity of the interaction by several orders of magnitude, and the term *avidity* is used to refer to the strength of these multivalent ligand interactions.[5] To fully understand the function of lectins, the kinetics of their multivalent interactions must be understood.

Galectins are one of the oldest class of mammalian lectins, and utilize multivalent interactions to perform their numerous functions. A major function of galectins is the regulation of immune and inflammatory responses, as well as triggering apoptosis.[6] Galectins bind to glycans terminating with galactose, but physiologically require lactose (composed of Galactoseβ1-4Glucose) or N-acetyllactosamine (LacNAc, composed of Galactoseβ1-4Glucosamine) for strong binding. Galectins can be prototypical, which contain a single carbohydrate-recognition domain and may associate to form homodimers. Galectins can also be chimeric, existing as a monomer or in a multivalent form, in which Galectin-3 is the only known vertebrate species. Like prototypical galectins, Galectin-3 has only one carbohydrate-recognition domain, but also has a large amino-terminal domain, which may allow for self-aggregation. Lastly, there are the tandem-repeat galectins which have two carbohydrate recognition domains, linked together by a small peptide domain. Additionally, many different isoforms can be found within these groups. The various galectin structures are presented in Figure 1.2.

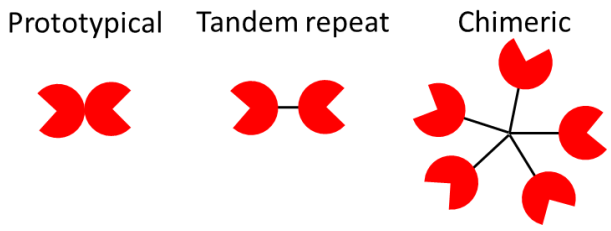

Figure 1.2: Different galectin structures. Galectin-1, -2, -7, -10, -13, and -14 are members of the prototypical group. Galectin-4, -8, -9, and -12 are of the tandem repeat group. Galectin-3 is the only known chimeric galectin, shown in the pentameric form.

The ability of galectins to associate and form higher order structures allow for multivalent interactions to occur. One interesting aspect of galectin binding is that dimeric galectin, such as those belonging to the prototypical and tandem repeat groups, can crosslink different ligands because the CRDs are located at opposite ends of the dimer. As an example, the prototypical Galectin-1 utilizes this feature to redistribute glycoproteins into segregated "microdomains" on the cell membrane, which in turn signals apoptosis of activated T-cells, as depicted in Figure 1.3. [7]

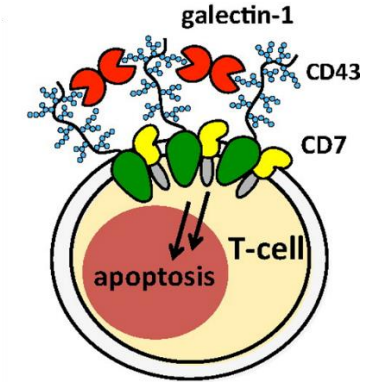

Figure 1.3: Schematic of Galectin-1 cross-linking inducing T-cell apoptosis. . Galectin-1 is known to induce apoptosis of human thymocytes and activated T-cells by binding to a set of T cell surface glycoproteins: CD45, CD43, and CD7. The cross-linking of the mucin glycoproteins CD43 and CD7 segregates the ligands on the cell surface into "microdomains," which signals apoptosis.[8]

The multivalency of lectins allows for multiple different type of binding interactions to occur, such as the bind-and-slide mechanism, where lectins are able to diffuse between carbohydrates on the same ligand.[9] The structures of lectin cross-linked with carbohydrates and glycoproteins have been studied, but the mechanisms of binding of lectins to glycoproteins that lead to cross-linking requires further study.[10,11]

Mannose-binding lectin (MBL), a C-type lectin belonging to the family of collectins, is an important member of the innate immune system. It contributes to antimicrobial immunity and protection by promoting opsonization and initiating activation of the classical complement system.[12] MBL interacts with the terminal mannose and fucose residues of glycans on the surface of micro-organisms to identify and neutralize the pathogen. Mammalian glycans do not typically terminate with mannose, which MBL utilizes to distinguish between self and non-self. MBL consists of three carbohydrate recognition domains that come together to form a dimer, with a tail of collagen-like helix that associates with another trimer to form a "dimer of trimers."[13] The interaction of MBLs multiple CRDs with multiple terminal mannose residues is essential for high-affinity binding, as the K_D is 1 mM with a high mannose oligosaccharide, and the K_D can be as low as 1 nM for a multivalent ligand.[13] To achieve the multivalent interactions necessary, the spacing of both the terminal sugar residues and of the independent carbohydrate recognition domains must be appropriate and fixed.

Methods for Analysis of Glycan-protein Interactions

Various techniques have been employed to evaluate multivalent glycan-receptor interactions, such as inhibition binding assays, isothermal titration calorimetry, or surface plasmon resonance, as well as many others. Surface plasmon resonance (SPR) is a technique in which either a ligand or a protein is immobilized on a sensor chip with a gold film. Either a ligand or a protein is then flowed over the chip as the analyte. The association of the ligand with the protein induces a change in the refractive index of the sensor chip, and from this information on the binding kinetics are obtained. A schematic of SPR is shown in Figure 1.4. This technique allows for rapid data collection of affinities ranging from mM to pM value using small volumes of analyte.

However, one drawback of SPR is that the analyte must have a mass large enough to cause a significant change in SPR upon binding. Because of this, the glycan is usually immobilized instead of the protein, which allows for the regeneration of the chip for reuse. Additionally, by altering the amount of glycan immobilized on the chip, conditions necessary for multivalent interactions could be evaluated. However, only one glycan condition can be measured per chip. Additionally, binding conditions are directly affected by the rate of mass transport of the analyte to the surface.[14] If the surface interaction consumes analyte faster than it is supplied, the measurement becomes a reflection of the transport of the analyte rather than the actual interaction.

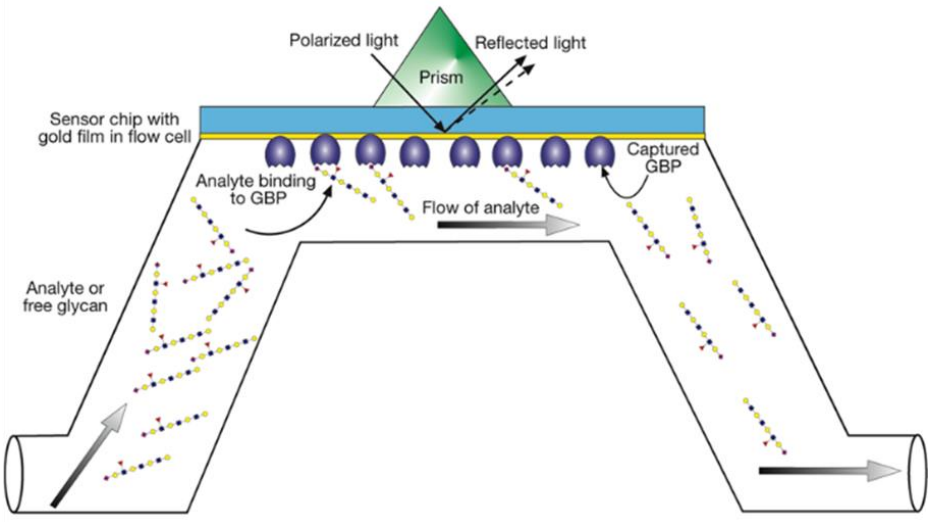

Figure 1.4: Schematic of SPR. Light reflected from a sensor chip with a gold film is measured and altered in response to the binding of free glycans to immobilized GBP.[5]

Isothermal titration microcalorimetry (ITC) is a method in which a solution containing a glycan of interest is added incrementally to a solution containing a fixed concentration of a GBP, and the heat generated from binding is measured relative to a reference.[5] This method has previously been used to evaluate galectin binding to asiaolofetuin (ASF), which is a glycoprotein that has nine LacNAc epitopes, and a schematic is depicted in Figure 1.5.[16] The galectins tested, Galectin-1, -2, -3, -4, -5, and -7, appeared to have a negative binding cooperativity to ASF, due to the decreased functional valency as the amount of galectins binding to it increases. While the binding thermodynamics are able to be determined, cross-linked complexes between the lectins and carbohydrates were not formed, as they determined ASF had almost the same degree of negative binding cooperativity with truncated Galectin-3 and Galectin-5 as their full-length molecules.

ITC is advantageous because all major thermodynamic information is collected. However, it may require large amounts of both protein and glycans, making this method both time and resource intensive to use for a wide range of glycans. Additionally, because the signal is proportional to the binding enthalpy, it can be difficult to obtain reliable data for weak interactions, due to the signal-to-noise ratio. The various methods used to evaluate multivalent glycan-receptor interactions are not rapid and high-throughput, making it difficult for the analysis of multiple glycan-binding proteins.

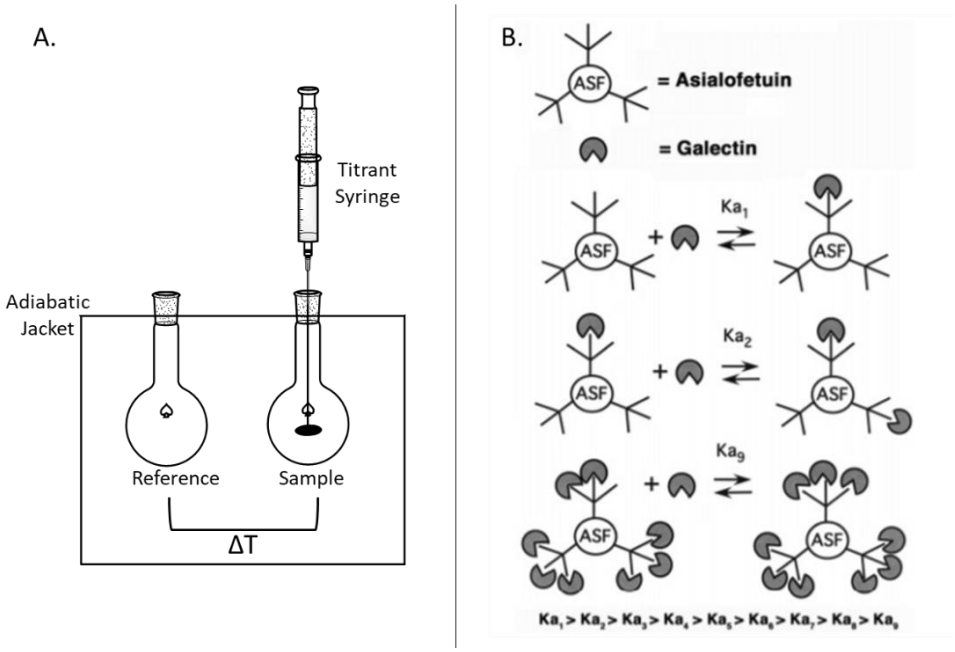

Figure 1.5: Isothermal Titration Calorimetry. A) General schematic of an isothermal titration calorimeter. B) Diagram of the various microequilibria constants for asialofetuin binding to multiple galectins.[15]

Glycan Microarrays

Microarrays originated as a high-throughput method of analyzing genes and gene products. Generally, glass chips are used as a substrate, with target elements placed on it in an ordered manner. Fluorescent probe molecules are then introduced, which would hybridize or bind to specific target molecules. The expression level could then be measured based on the intensity of fluorescent signal.[16] The first microarrays were generated via robotic printing of complementary DNA on glass, which were then used for quantitative expression measurements of corresponding genes.[17] This method was quickly adapted to create protein arrays capable of: screening for protein-protein interactions, identifying protein kinase substrates, and identifying the protein targets of small molecules.[18] The proteins can be covalently bound by treating slides with an aldehyde-containing silane reagent, which react with primary amines on proteins to form Schiff's base linkages. Using this method, the proteins are attached nonspecifically and could be bound in a variety of orientations. Due to the uncontrolled orientation in immobilization, this method of attachment is not ideal for proteins that have a specific ligand recognition domain. The development of glycan microarrays came soon after the advancement from DNA to protein arrays, due to the need for a high-throughput method of determining glycan-binding protein specificities. In the years since the development of the first glycan microarrays, numerous methods of immobilization have been developed, from noncovalent non-site specific to covalent and site-specific, displayed in Figure 1.6.

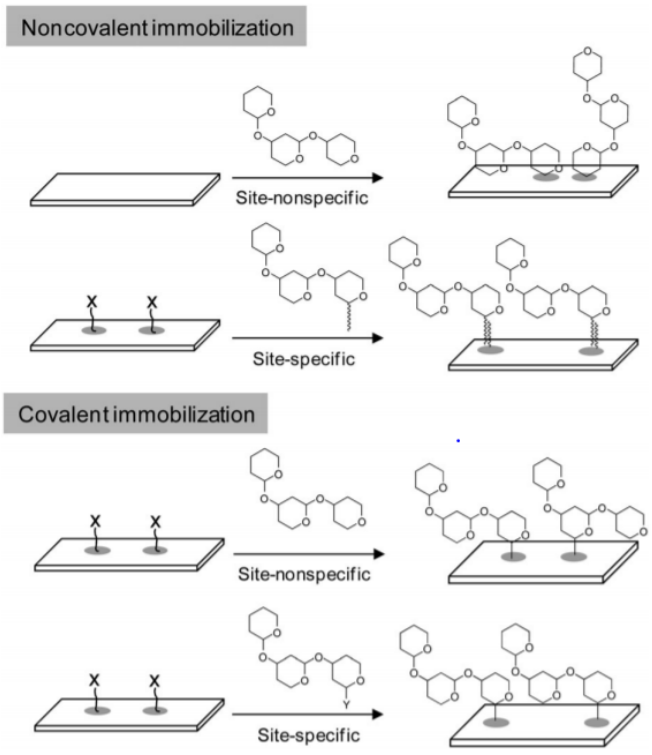

Figure 1.6: Glycan immobilization strategies for the construction of microarrays Glycan microarrays can be divided into two groups: noncovalent immobilization shown on top, and covalent immobilization shown on the bottom. These groups can be further subdivided based on the site-specific or nonspecific manner of attachment.[19]

Non-covalent, site-nonspecific was one of the first methods used for glycan immobilization. It most commonly employs nitrocellulose-coated glass slides in which glycans are adsorbed to the surface, with the degree of adsorption dependent on the hydrophobicity and size of the glycan.[19] To minimize the loss of glycan during the washing step, the glycan must be large enough to sufficiently adsorb to the surface, while also being hydrophobic enough to not wash away in an aqueous solution. One of the first methods of creating these glycan microarrays was by spotting fluorescein isothiocyanate-conjugated α(1,6)dextran onto nitrocellulose polymer coated glass slides.[20] Dextran, which are glucose polymers, were shown to be noncovalently immobilized, with larger

(2,000 kDa) dextran showing improved retention over smaller (20 kDa to 70 kDa) dextran. The reactivates of immobilized carbohydrates was also tested by printing dextran of different linkage compositions, which were then incubated with monoclonal antibodies of defined specificities.[20] While useful for studying general binding specificities, this platform does not allow for the characterization of binding, as the orientation of glycans on the surface is unknown.

Non-covalent site-specific methods of glycan immobilization have also been developed. The interaction between biotin and streptavidin can be used to immobilize biotin-conjugated glycans onto streptavidin coated slides. The first use of biotin-streptavidin interactions was in the comparison of glycan microarrays to ELISA, in which both methods showed similar results for the specificity of antibodies to carbohydrate antigens, providing some early validation to the use of microarrays.[21] Covalent and site-nonspecific immobilization of glycans have also been employed, mostly using photoreactive groups. This one-step method of immobilization has the added benefit of employing unmodified glycans, but is inherently flawed due to the nonspecific immobilization, as the overall orientation of the glycans is unknown.

The first technique for the covalent and site-specific attachment of monosaccharides was achieved shortly after the advent of glycan microarrays. Carbohydrate-cyclopentadiene conjugates were synthesized via the activation of cyclopentadienyl carboxylic acid with isobutylchloroformate and couple with an aminoglycoside, which was spotted onto a monolayer presenting benzoquinone groups allowing for the covalent immobilization via Diels-Alder cycloaddition.[22] This provides

numerous benefits, including the ability to normalize the density of immobilized carbohydrates, since it is not dependent on the structure of the carbohydrate. This method also allows for specific presentation of the monosaccharide on the surface, but it does not effectively mimic the native structure of glycans, as some lectins are specific for not only the terminal carbohydrate, but also subsequent ones. Additionally, side chains and branched motifs found in native glycans are not replicated in this method, which can affect avidity of lectin binding which is dependent on the spacing of the glycans.

The covalent site-specific method of immobilization is likely the most explored method of glycan attachment, despite the need to modify sugars, which can be intensive.[19] Numerous methods have been employed, including: sulfhydryl-maleimide conjugation[23], diels-alder reaction[24], Staudinger ligation[25], N-hydroxysuccinimide (NHS) ester crosslinking with amine[26], and azide-alkyne reactions.[27] Examples of the many different types of covalent and site-specific methods of immobilization are shown below in Figure 1.7.

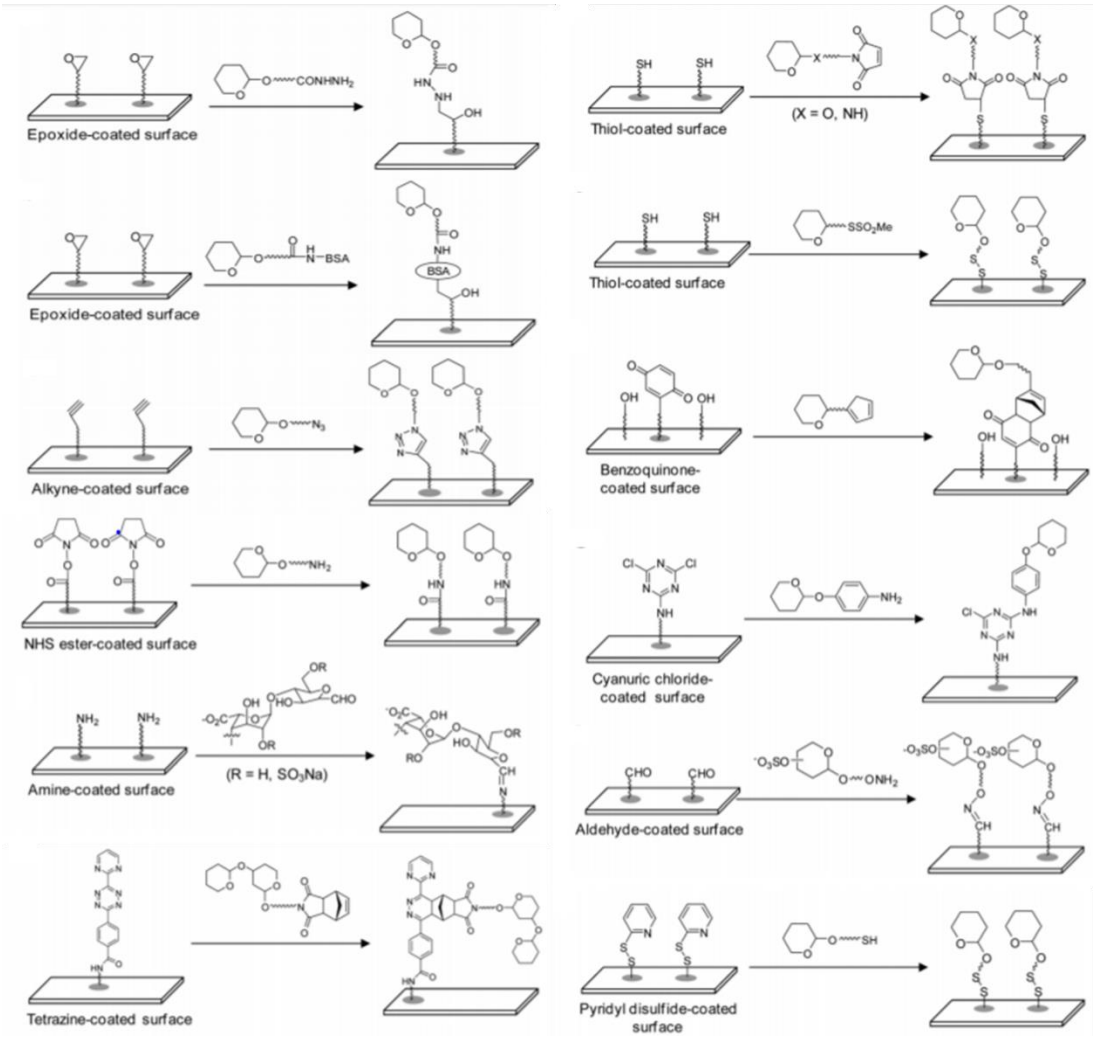

Figure 1.7: Different methods of constructing covalent, site-specific glycan microarrays. Numerous techniques to create both covalent and site-specific glycan microarrays have been developed, using a wide variety of surface coatings.[19]

Covalent and site specific methods have been developed that do not require sugar modification, but require either an aminooxy- or hydrazide-coated surface, resulting in both acyclic and cyclic forms of the sugars, which has a negative impact on protein binding.[28] While allowing for the analysis and quantitative determination of glycan-protein binding, the amount of glycan attached to the surface cannot be directly measured. Without knowing the amount of glycan on the surface, and thereby an

estimation of the spacing between each glycan, it becomes difficult to accurately measure the binding affinities of multivalent interactions. To assess multivalent interactions, both the monomeric and multimeric forms of the glycan-binding protein require evaluation and comparison. Even still, differences in protein sizes between the monomeric and multimeric forms could account for some differences in binding affinity. For accurately measuring multivalent interactions, the amount of glycan on the surface must be known, and the glycan spacing and orientation must also be controlled.

A method for determining multivalent interactions was previously reported using glycans with an amine attached to the anomeric position printed onto an NHS-coated glass slide.[29] To determine the surface coverage of printed glycans, fluorescein isothiocyanate (FITC) cadaverine was used as a model. This method is inadequate for accurately determining the "true" surface coverage, as the grafting of glycans and of FITC cadaverine to the surface is likely different. Despite varying concentrations of the monosaccharide mannose from 10 μM to 100 μM, the apparent K_D was closely distributed, with a mean of 83 nM and a standard deviation of 4.7 nM. Once the printing concentration of glycan is lowered to 1 μM and 0.6 μM, the apparent K_D increases to 221 nM and 214 nM, respectively. While there is a decrease in binding affinity, because the apparent K_D is still in the nanomolar range it is possible there are still some multivalent binding occurring.

Quantification of glycan-protein interactions is typically done by incubating the protein of interest at a variety of concentrations. The protein concentration is then plotted against the fluorescence intensity for each of the conditions tested.[47] This creates binding

curves, which are then analyzed as Langmuir isotherms to generate the apparent K_D. The formation of the ligand-protein complex, LP, on the slide surface between the surface ligand (L) and protein of interest (P) is considered the bimolecular reverse reaction scheme (Figure 1.8).[48,49] As described by Liang, et. al., the Langmuir isotherm used for microarrays can be derived as follows. The rate of complex formation is:

$$\frac{d[LP]}{dt} = K_a[L][P] - K_b[LP]$$

The difference between the total amount of ligand, $[L_T]$ and the amount of [LP] is the amount of unoccupied ligand [L] remaining.[49] Substituting this into the previous equation gives:

$$\frac{d[LP]}{dt} = K_a[P]\left([L_t] - [LP]\right) - K_b[LP]$$

The $[L_T]$ can be described in terms of the maximum analyte binding capacity of the surface, F_{max}, and the [LP] can be described as the fluorescence binding signal, F.[49] Substituting this gives the following:

$$\frac{d[F]}{dt} = K_a[P](F_{max} - F) - K_b[LP]$$

When at equilibrium, where apparent $K_D = K_b/K_a$ and $d[F]/dt = 0$, the apparent dissociation constant can be obtained via the following formula.[49]

$$F = \frac{F_{max}[P]}{[P] + K_D}$$

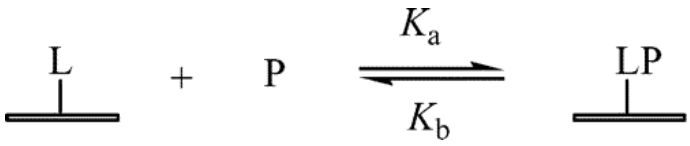

Figure 1.8: The bimolecular reversible reaction scheme of ligand-protein complex formation. L represents the surface-bound ligand, whereas P is the protein of interest, and LP is the ligand-protein complex formed. The association rate constant, K_a, has units of concentration^{-1} time^{-1} and dissociation rate constant, K_b, has units time^{-1}. At equilibrium, the ratio of free ligand L and unbound protein P to the ligand-protein complex LP is the dissociation constant.[48,49]

The presentation of the glycans on the slide surface plays a large role in the ability of lectins to bind to the glycans. This includes the distance of the glycan from the surface of the slide. Carbohydrates have previously been coupled to maleimide with varying tether lengths and printed onto a thiol-coated surface, as shown in Figure 1.9. The length of the tether appeared to influence lectin binding affinity, with lectins binding weakest (~5 mM) to glycans coupled to the shortest linker, while glycans coupled to longer linkers showed similar binding affinities at glycan concentrations as low as 0.5 mM.[23]

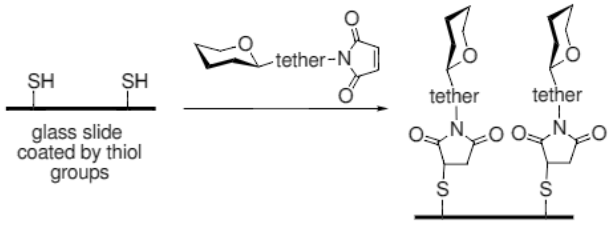

Figure 1.9: Schematic of the immobilization of maleimide-linked glycans onto thiol-coated slides. Tethers of various lengths were used to attach maleimide to glycans, which were then printed onto a thiol-coated surface. The length of the tether appeared to have an impact on lectin binding, as glycan with the smallest tether bound to lectins weaker compared to glycans attached with the longer tethers.[23]

Well-defined glycan structures that can be employed to probe lectin-glycan interactions could possibly be achieved by mimicking natural glycoproteins using synthetic glycopolymers. Glycopolymers of average repeating units ranging from 10 to

143 have previously been synthesized to determine the effect polymer chain length and flexibility have on the functional affinity of the glycopolymers with the mannose-binding tetrameric lectin concanavalin-A in a agglutination assay.[9] As shown in Figure 1.10, the potencies of the glycopolymers increased exponentially as the polymer average length increases until it plateaus at 50 repeating units, and all multivalent mannose ligands had an increase in binding compared to a monovalent mannose. From this, it can be concluded that increasing the average polymer length allows for more of the population of concanavalin-A to span the distance between two mannose binding sites. At polymer lengths with more mannose residues than needed, the rebinding of concanavalin-A becomes more favorable than the dissociation due to the readily availability of the other mannose residues. More generally, glycopolymers can be used to investigate multivalent recognition through determining the optimal length, as well as the optimal number of ligands necessary.

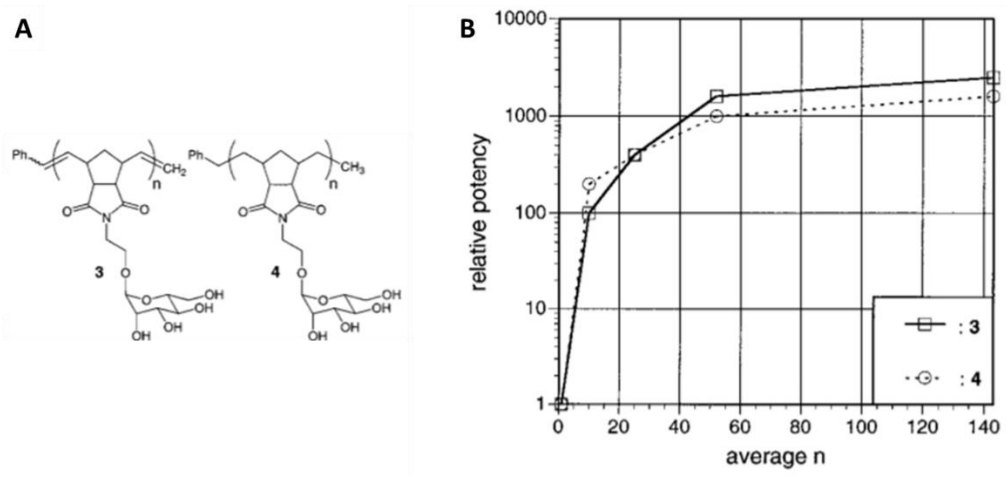

Figure 1.10 Determination of polymer chain length on the functional affinity of concanavalin-A with mannose. A) Structure of the mannose glycopolymer (**3**: saturated, **4**: unsaturated) synthesized via ring-opening metathesis polymerization. The average number of repeating units, n, studied were 10, 25, 52, and 143. B) The interaction between polymer length and hemagglutination inhibition. The relative potencies is defined as [inhibitory dose of polymer bound mannose]/[inhibitory dose of monovalent mannoside].[9]

One interesting method is the conjugation of glycans to a carrier protein, which is often bovine serum albumin (BSA), that is used for attachment to an epoxide surface. A representation of this is shown in Figure 1.9. The conjugation of glycans to BSA can be accomplished in numerous ways, such as the reductive amination of lactols or by coupling to linkers attached onto carbohydrates, and generally take advantage of evenly distributed free amine groups on BSA.[30]

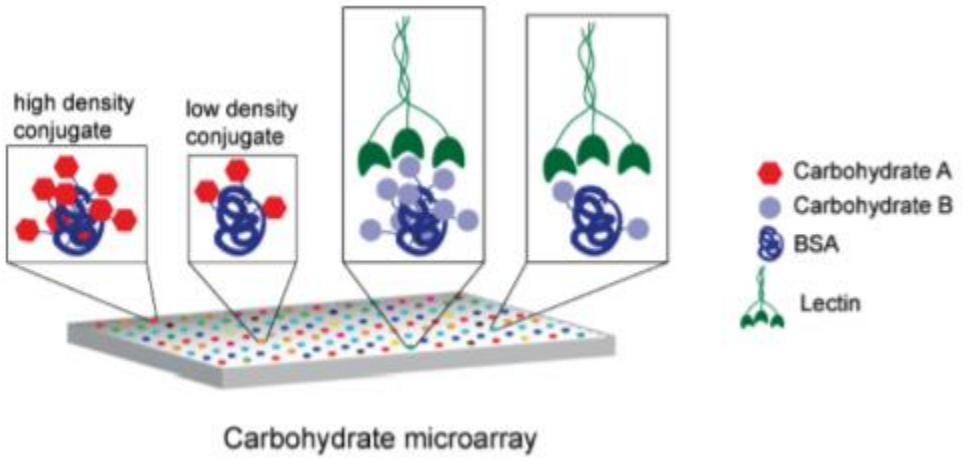

Figure 1.11 Altered glycan density of glycan-BSA conjugates. Glycan-BSA conjugates can be created in a density-variant manner and printed onto epoxide-coated slides. The binding of lections can then be studied to evaluate the effects of density on binding affinity.[31]

This method of forming glycan-BSA conjugates has been used to determine the valency-dependent binding properties of lectins and monoclonal antibodies.[31] Altering the number of carbohydrates attached to BSA allows for the generation of high or low valency glycan-BSA conjugates, and the use of linkers allows for some separation of the glycan from the protein. The amount of glycan on the surface can be approximated by determining the valency of glycan per BSA, based on MALDI-TOF MS, and by determining the amount of glycan-BSA conjugate present on the surface via an additional conjugation with a fluorophore. However, the glycan conjugation is not done in a site-specific manner, and the space between each glycan could be very different for each unit of BSA at a specific valency. While multivalent interactions and density-dependent binding curves were generated, the glycans present on the array are likely not presented in a biologically relevant manner. The glycan-BSA conjugates are printed onto an epoxysilane slide and nonspecifically immobilized. Due to this, the amount of actual

glycan available and presented for binding are likely less than the actual amount of glycans on the glycoconjugate, and the dissociation constants should be determined using an alternative method to ensure the results of the glycan-BSA conjugate are accurate.

Glycopolymers designed to mimic mucins for use in microarrays have previously been developed. The polymers were comprised of three domains: a central mucin mimetic domain, where the glycans are displayed, a terminal domain functionalized with an alkyne group for covalent immobilization, and a second terminal domain labeled with a fluorophore, Texas Red.[32] The central mucin mimetic domain was designed with ketones for the condensation of aminooxy glycans, The glycopolymers were then microcontact printed onto silicon wafer chips with surface azido groups via a poly(dimethylsiloxane) stamp that was inked in a solution of the glycopolymer, copper sulfate, and tris[(1-benzyl-1H-1,2,3-triazol-4-yl)methyl]amine (TBTA) and sodium ascorbate in 1:1 water and DMSO. By printing in the presence of copper, the terminal alkyne on the glycopolymers reacted with the surface azides and fluorescence was still present after extensive washes. When printed without the copper catalyst, no fluorescent signal remained, indicating the polymer was washed away, and the glycopolymers are covalently attached to the surface when printed in the presence of copper, as shown in Figure 1.11. A lectin, *Helix pomatia* agglutinin, bound to the printed glycopolymers in a glycan-specific manner, only binding to a GalNAc-modified polymer. Binding was inhibited in the presence of free 200 mM GalNAc in the binding solution.

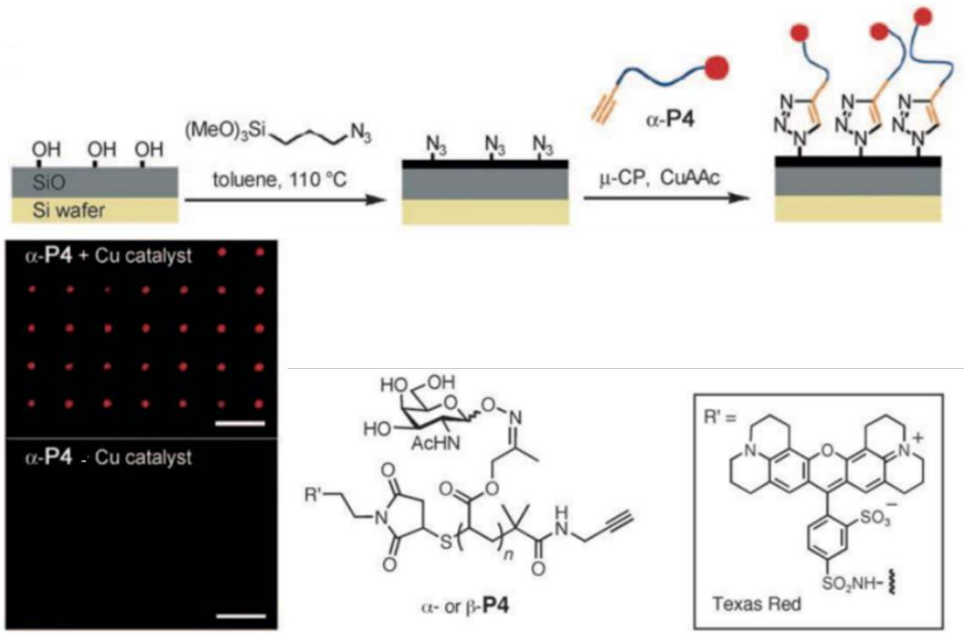

Figure 1.12: Method of covalently attaching glycopolymers to an azide-terminated silicon wafer. The glycopolymers were printed in a solution containing copper-click reagents onto a silicon wafer coated with azides. After extensive washes of the wafer, a fluorescent signal from a fluorophore attached to the polymer is still able to be detected. When printed without a copper catalyst, no fluorescent signal is present.[33]

Glycopolymer microarrays were later employed to evaluate the cross-linking binding method of lectins. The ability of lectins to cross-link and bridge adjacent ligands is dependent on optimal spacing of the ligands themselves. Increasing the distance between the ligands on the surface of the slide, accomplished by lowering the concentration of glycopolymer printed, would limit the lectins ability to cross-link. This change in binding mode would be reflected in the K_D of the lectin. If the lectin cross-links multiple ligands, the K_D would be higher in low-density arrays. Glycopolymer mimetics, whose structure is shown in Figure 1.12, was printed at concentrations ranging from 400 nM to 75 nM onto streptavidin-coated glass slides in 100 mM aqueous sodium phosphate with 0.01% BSA and 1.5 M betaine, a zwitterion.[33] Dissociation constants of four lectins:

G. max, *W. floribunda* lectin, *V. villosa* agglutinin, and *H. pomatia* agglutinin, were then determined at each of the printed concentrations.

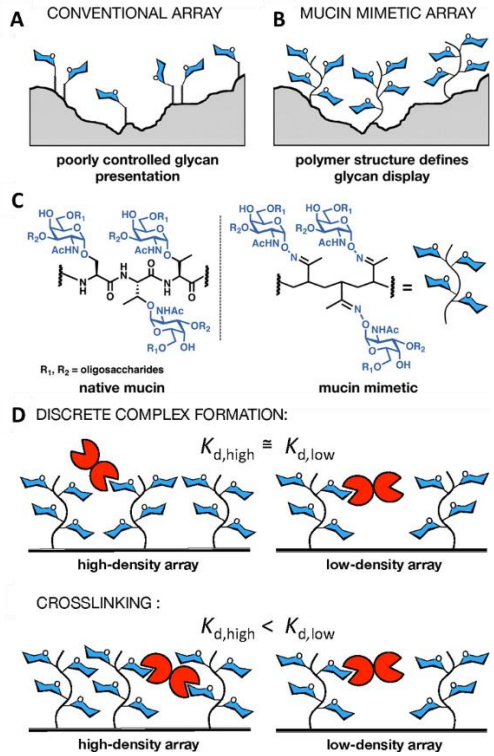

Figure 1.13: Schematic of the glycopolymer used to evaluate lectin binding. A) Figure of the conventional presentation of glycans on a microarray slide. B) Using glycopolymers, the glycans are presented on a polymer backbone attached to the surface of the microarray slide. This allows for the control of glycan presentation, as well as mimicking the natural presentation of glycans. C) Pictured on the left is a general schematic of a native mucin with a core sugar α-*N*-acetylgalactosamine. On the right is the glycopolymer mimetic, created via the oxime ligation of α-aminooxy-GalNAc to a poly(methylvinyl ketone) backbone. D) Determination of lectin cross-linking using polymer density-variant microarrays. If the lectin of study does not cross-link glycans, then the expected K_D of the lectin on both high-density polymer arrays and low-density polymer arrays are expected to be similar. If the lectin of study does cross-link glycans, then the expected K_D of the lectin on high-density polymer microarrays, under conditions favorable to cross-linking, is expected to be much lower than on low-density polymer microarrays, where the distance between each polymer is too great for the lectin to cross-link.[34]

Glycopolymer arrays show much promise in the ability to analyze the lectin cross-linking and multivalent binding affinity in a high-throughput manner. However, more

emphasis needs to be placed on evaluating both the length, valency, and concentration of glycopolymer on the slide surface. Manipulating the valency of the polymer will alter the spacing of the sugar on the polymer itself, whereas altering the concentration of glycopolymer printed onto the surface will alter the spacing of the glycopolymer on the surface, allowing for the determination of optimal spacing needed for crosslinking interactions to occur. Finally, altering the polymer length but maintaining a constant glycan valency allows for the control of the density of glycan on the polymer itself. This permits the study of multivalent interactions on the same polymer.

Different technology for printing glycan solutions onto the surface have similarly been developed, and generally fall into contact printing, utilizing steel pins dipped into glycan solutions and printed directly onto the surface, and non-contact printing, which uses a piezo-electric printer to control the amount of the glycan solution to deliver from a capillary tip to the surface.[34] While contact printing does allow for spot reproducibility, the amount of solution delivered is dependent on the amount of time the pin is in contact with the surface, and is not independently controlled. Depending on the non-contact printer, it becomes possible to control the amount of solution delivered to the surface, as well as the concentration delivered. However, the non-contact printer is limited by the amount of relatively delicate tips it can use at a time, and as such the factor of time must be taken into consideration when determining what substrate, temperature, and humidity should be used for the microarray print.

Aims

The main objective of this work is to develop a density-variant glycan microarray using the current lab mucin mimetic glycopolymer. The current glycopolymer allows for a more native presentation of glycans on the array surface. Fluorophore labeling of the glycopolymer will allow for the determination of relative glycan on the surface. These glycan microarrays will be developed to understand the method of multivalent interaction employed by a lectin, such as crosslinking employed by galectins. In order to accomplish this, numerous factors must be analyzed. The first is the spacing of glycopolymers attached to the surface, controlled by the concentration of glycopolymer spotted onto the slide surface. This will uncover the spatial separation needed for lectin crosslinking to occur, as the CRDs must be able to reach their respective ligands. The second factor is the valency of glycan on the polymer, which will determine the amount of glycan needed for optimal lectin binding. Finally, the length of the glycopolymer itself will be modulated, which can control the density of glycan on the glycopolymer. This will alter the spacing of the glycan on the polymer itself, as well as allowing a broad range of glycan valency to be tested.

The density-variant glycan microarrays will be initially evaluated using the lectin *Ricinus communis* agglutinin I (RCA_{120}). which is a commonly studied lectin that preferentially binds β-linked galactose. RCA_{120} is a member of the R-type lectins of approximately 120 kDa, and exists as a tetramer of two noncovalently associated heterodimer-like proteins.[50] Both heterodimers contain a toxic A-chain linked to a galactose-binding B chain via a disulfide linkage. The affinity of RCA_{120} for

monosaccharides is low, (K_D range of 10^{-3} to 10^{-4} M), but binds to cells with a higher affinity (K_D range of 10^{-7} to 10^{-8} M).[50] This is due to the increased binding to glycans terminating with Galβ1-4GlcNAc, as well as because of increased avidity due to multivalency

II. Methods

Synthesis of Glycopolymers

Glycopolymer synthesis was done as previously reported.[35] Azide-terminated acrylamide polymers were added to a Schlenk flask, placed under nitrogen, and 0.705 mL of a degassed 20 mM *n*-butylamine solution in THF was added at 0 °C and allowed to react for 2 hours. The reaction mixture was diluted in ether and precipitated in hexanes via centrifugation (1000 xg, 3 min.), which was repeated three times. To remove residual hexanes, the polymer was concentrated from DCM three times and then dried under vacuum.

End-deprotected polymers were dissolved in a 2 mM TAMRA Cy_5-maleimide (1.5 eq) solution in DMF (anhydrous). The mixture was degassed and allowed to react overnight, covered. The reaction mixture was precipitated in hexanes three times, and the remaining polymer was concentrated from DCM three times before being dried under vacuum. The fluorophore labeled polymer was placed under nitrogen and dissolved in a freshly prepared solution of TMS-Cl (1 M) and phenol (3 M) in DCM (anhydrous). The reaction mixture was allowed to react for 2 hours, and the side-chain deprotected polymer was precipitated in ether three times. The amount of polymer labeled by TAMRA was determined by weighing out a small amount of lyophilized fluorophore labeled polymer and dissolving in a known amount of deuterated phosphate-buffered saline (PBS). Final NMRs are shown in Appendix Figure 6.1.

Sugar Ligation

The fluorophore-labeled and side-chain deprotected polymer was dissolved in a sodium acetate buffer (1 M NaOAc, 1 M urea, pH=4.5) to form a 200 mM by side-chain solution.[35] Glycan was added to the solution ranging from 1.1 eq to 0.2 eq, depending on the desired valency of the glycopolymer. The reaction mixture was heated in a thermocycler at 50°C for 72 hours. The mixture was then spin dialyzed (6000 xg, 14 min.) with an Amicon 10 KDaUltra Centrifugal Filter (equilibrated with 500 μL of Milli-Q water twice by spin dialysis) four times with 500 μL of deuterated phosphate buffered saline solution (100 mM phosphate, 150 mM NaCl, pD 7.4). The spin column was then inverted into a clean centrifuge tube, and the polymer solution was collected via centrifugation (300 xg, 1 min.) and analyzed by ^{1}H NMR. The ^{1}H NMR for each polymer is shown in the Appendix Figure 5.1. The sugar ligation efficiency was calculated by subtracting polymer backbone protons from the total integration of the region δ2.5-4.5 ppm and then dividing by the number of glycan protons.

Cyclooctyne Slide Preparation

Cyclooctyne Microarray slides were prepared as previously described.[35] Epoxysilane glass slides (Thermo Scientific SuperChip Microarray Slides Cat. # C50-5588-M20) were incubated overnight at room temperature while rocking in a 1 mM solution of dibenzocyclooctyne-amine and 100 μL of DIPEA per 10 mL of anhydrous DMF. The slides were then removed and sonicated in methanol twice for 15 minutes, rinsed with Milli-Q water, and "spin-dried" via centrifugation at 500 rpm for 5 minutes. The slides were then stored at 20°C with desiccant until used.

Propargylamine Slide Preparation

Epoxysilane glass slides were incubated overnight with rocking in a solution of freshly distilled 1 mM propargylamine and 100 μL of DIPEA per 10 mL of anhydrous DMF. The slides were then sonicated in methanol twice for 15 minutes each, rinsed with Milli-Q water, and "spun-dry" at 500 rpm for 5 minutes each, and then stored at 20°C with desiccant.

DiaminoPEG Slide Preparation

Epoxysilane slides were added to a solution of 1 mg/mL of poly(ethylene glycol) bisamine with an average M_n of 10,000 in 0.8 M K_2SO_4 and 0.1 M Phosphate Buffer at a pH of 6.4.[36,37] The solution was heated to 60°C in a water bath, upon which the solution reached cloud-point and was allowed to react for 12 hours. The slides were washed in 1X PBS three times for fifteen minutes with rocking, then rinsed with Milli-Q water and "spin-dried" at 500 rpm for 5 minutes. The slides were then stored at 20°C in desiccant. The poly(ethylene glycol) bisamine in solution was able to reach cloudpoint for multiple rounds of slide functionalization, and was used until the solution was unable to reach cloudpoint.

EDC Coupling of propargylic acid to poly(ethyleneglycol) bisamine slides

Poly(ethyleneglycol) bisamine slides were placed into a solution of 0.1 M propargylic acid, 0.1 M acetic acid, 0.1 M sodium phosphate monobasic, and 10 mg/mL of 1-Ethyl-3-(3-dimethylaminopropyl)carbodiimide hydrochloride at pH = 5 and allowed to react overnight while rocking.[38] The slides were then washed in 1X PBS three times

for fifteen minutes, then rinsed in Milli-Q water and “spun-dry” at 550 rpm for 5 minutes. The slides were then stored at 20°C.

Contact Angle Measurements

Contact angle measurements of functionalized slides were taken using a ramé-hart model 190 Contact Angle Goniometer, with DROPimage CA software. One drop of water was placed onto the slide, and the complementary angles were collected at various horizontal limits. This was repeated on each quadrant of the slide, with 50 contact angle measurements taken for each drop placed on the slide.

Slide Passivation

Unless otherwise stated, slides were passivated in a filtered 1X PBS solution with 1% Bovine Serum Albumin (BSA) and 0.1% Tween-20 at a pH of 7.4 for one hour with rocking. The slides were then removed from the passivation buffer and washed with 1X PBS solution three times for fifteen minutes, then rinsed in Milli-Q water and “spin-dried” and immediately used for printing. Alternative passivation buffers were also used in which BSA was substituted for Casein, and the concentration of both was varied from 0.1% to 10%.

Ethanolamine/Borate Passivation

Prior to typical passivation, slides were placed in a solution of 94 mM sodium tetraborate (9.5 g) and 98 mM ethanolamine (3.00 g) in 500 mL of Milli-Q water at a pH of 8.5. Once slides were submerged, the container was covered and allowed to rock for

three hours. Afterwards the slides were washed in Milli-Q water for 10 minutes with rocking, and then immediately placed in the 1% BSA passivation solution.

Microarray Printing

Glycopolymers were initially printed using a sonoplot GIX microplotter desktop non-contact printer equipped with a piezo-electric dispenser tip. Final prints were done using an ArrayIt SpotBot Extreme Microarray Spotter printer, courtesy of the Varki lab. Glycopolymers were printed in a 1X PBS-derived printing buffer, with final optimized printing conditions containing 0.1% BSA and 0.05% glycerol at a humidity of 75%. The propargylamine test prints utilized numerous different printing buffers, and the concentrations for each component is as follows: 0.1 μM $CuSO_4$, 1 μM Sodium Ascorbate, 1 M NaCl, 0.2 μM Tris(benzyltriazolylmethyl)amine (TBTA), 1:2 *tert*-Butyl alcohol:PBS, and a few drops of dimethyl sulfoxide to dissolve the TBTA, and finally 0.05% glycerol. The glycopolymers were serially diluted starting from either 15 μM or 10 μM down to a concentration of 0.1 μM to 0.001 μM, depending on the desired arrays. Printed microarrays were analyzed using an Axon GenePix 4000B microarray scanner (Molecular Devices) equipped with a Cy3 and Cy5 filter at PMT voltage settings where saturated pixels were no longer obtained. After printing, the slides were re-humidified using steam from Milli-Q water, and then "snap-dried" on an 80°C glass plate. The slides were imaged and allowed to react overnight at 20°C. The slides were vigorously dunked in a 0.1% Triton-X, 1X PBS solution for 2 minutes, then washed in a 0.1% Triton-X, 1X PBS solution for 15 minutes with rocking. The slides were then washed in 1X PBS twice for 10 minutes with rocking, then rinsed in Milli-Q water, spun-dried, and imaged.

Lectin fluorophore labeling

Lectins were labeled in a 5 mg/mL solution of the appropriate lectin with NHS-Ester Alexafluor-647 in 10 mM HEPES, pH of 8-8.4, containing 0.5 M Lactose to protect the binding site from labelling. The mass of NHS-Ester AF-647 added to the reaction mixture was calculated from the following equation:

$$10(\text{eq})\ \text{X Protein mass X}\ \frac{\text{M.W.}_{\text{NHS}}}{\text{M.W.}_{\text{Protein}}} = \text{NHS ester mass}$$

The solution was allowed to react for 4 hours at room temperature. After completion, excess fluorophore was removed via a PD-10 column and filtered using a 10 K Amicon spin filter centrifuged at 3000 xg for fifteen minutes at 4°C, washing with lectin storage buffer twice (For RCA_{120}: 10 mM phosphate, 0.15 M sodium chloride, pH of 7.5, with 0.08% sodium azide; for PNA: 10 mM HEPES, pH 7.5, 0.15 M sodium chloride, 0.08% sodium azide, 0.1 mM Ca^{2+}, 0.1 mM Mn^{2+}). The concentration of labeled lectin was calculated based on the following formula, with the correction factor for RCA_{120} being 0.236:

$$[\text{Labeled lectin}] = \frac{\text{Abs}_{280} - (\text{Abs}_{650} * \text{Correction Factor})}{\text{e}} * \text{Dilution Factor}$$

Lectin Binding Assays

Prior to performing each binding assay, lectins were purified on a Lactose-Agarose gel (Vector), washed with the appropriate storage buffer four times, and finally eluted in a lectin binding buffer (LBB) consisting of 1X PBS, 0.9 mM Ca^{2+}, 0.4 mM Mg^{2+}, and 0.2 mM Mn^{2+} containing either galactose or lactose at concentrations ranging from 100mM to 500mM. Well-gaskets were placed around previously printed and

washed arrays, which were then washed with LBB three times to, followed by blocking in a 1% BSA/PBS solution for 20 minutes, and then rinsed with 1% BSA/LBB three times. Lectin solutions diluted in LBB were then aliquoted into each gasket, and allowed to bind for one hour. Arrays were washed with 1% BSA/LBB three times, and then rinsed with Milli-Q water, spun-dry, and imaged. Binding curves were graphed using GraphPad Prism 7.02, and apparent K_D values were determined using the one site – specific binding, and calculated using the following formula:

$$F_{635} = \frac{F_{max}[P]}{[P]+K_D}$$

III. Results

The initial method for generating glycan microarrays was adapted from previous procedures performed in the lab.[35] In brief, Epoxysilane Superchip glass slides were functionalized with dibenzocyclooctyne-amine and azide-functionalized glycopolymers were printed at a range of concentrations. The glycopolymers are generated via RAFT polymerization, and the synthesis depicted in Figure 3.1. The distance between each polymer is increased by decreasing the concentration of polymer printed in the array. This allowed for the potential study of lectin cross-linking events based on the distance between the polymer printed in each spot on the array.

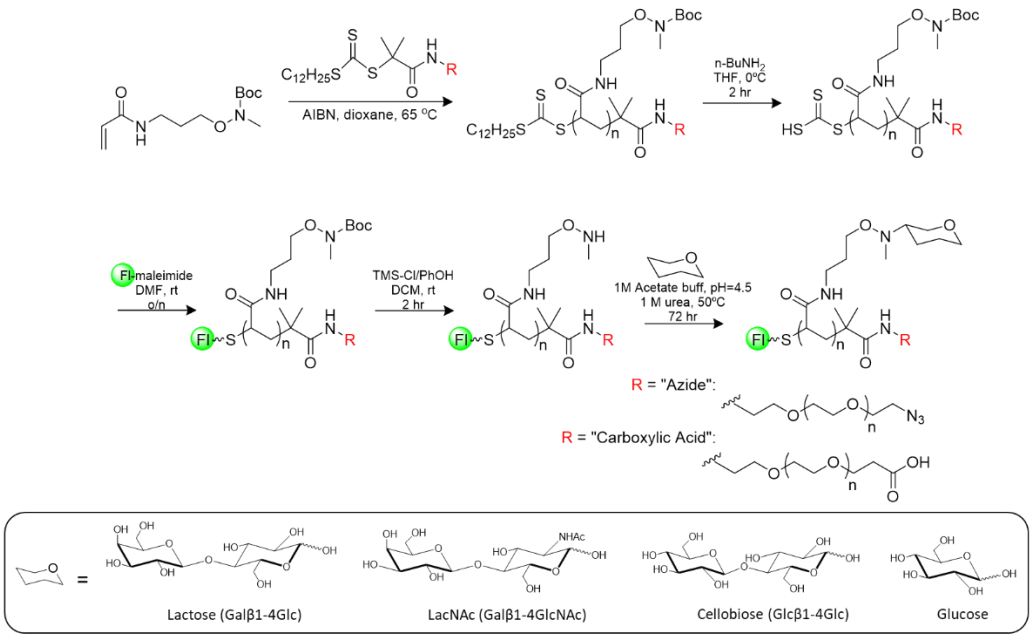

Figure 3.1: Schematic of the glycopolymer generation. An acrylamide-based monomer was polymerized via RAFT polymerization, followed by fluorophore labeling, side-chain deprotection, and sugar ligation of Lactose, LacNAc, Cellobiose, and Glucose.

When developing density-variant glycan arrays, consideration must be given to the amount of glycan on the polymer and the length of the polymer to assess the optimal glycan spacing for lectin binding. Polymer precursor backbones of varying lengths, defined as the number of repeating units of the polymer and represented by the "n" value, were previously synthesized in the laboratory, end-deprotected to release a reactive thiol group, and labeled with TAMRA. The labeling efficiencies, determined via UV-VIS spectrophotometry, are shown in Table 3.1. The n=424 polymer was borrowed from another colleague, Taryn Lucas, already labeled with TAMRA and ligated with the glycan lactose for use in the final microarray generation and lectin binding experiments.

Table 3.1: Efficiency of fluorophore labeling on each polymer. Labeling efficiency for was obtained by UV-VIS spectrophotometry of a sample of each polymer at a known concentration.

Polymer	% Fluorophore Labeling
Azide Polymer n=212	27%
Azide Polymer n=150	20%
Carboxylic Acid Polymer n=273	27%
Azide Polymer n=424	9.3% 13%

Various sugar ligation reactions were completed by altering the molar equivalents of glycan added to the polymer solutions (held constant at 200 mM with respect to N-methylaminooxy side-chains). This method effectively allowed for the establishment of glycan valency, which is defined as the number of glycans ligated to the polymer chain. Varying the glycan valency of each polymer, as well as the identity of the glycan can provide information regarding the optimal density of glycans on the polymer for lectin binding and crosslinking.

Four sugars were chosen: Lactose (Lac), N-acetyllactosamine (LacNAc), cellobiose, and glucose (Glc). Lactose and LacNAc were chosen for their ability to bind to lectins of interest, such as various galectins, as well as the commonly studied lectin *Ricinus Communis* Agglutinin (RCA_{120}). Except for two ligation reactions, Lac typically showed a higher ligation efficiency at each equivalence than LacNAc, as shown through the valency in Figure 3.2. The polymer of length n=212 was used for initial experiments for printing optimization, and had an increased number of glycopolymers to determine the reaction efficiency. For later experiments, the range of valency was lowered to generate glycopolymers with only high and low valency. A table of the valency of each polymer is shown in the Appendix Table 6.1. Polymer lengths of n=212, n=150, and n=424 were chosen to determine the effect glycan spacing on the polymer itself has on lectin binding. The Azide 129 Lac n=424 glycopolymer has a similar valency to the Azide 110 Lac n=150 glycopolymer, however the spacing of the Lac on each glycopolymer is vastly different. This allows for the determination of ideal glycan spacing for optimal lectin binding. The valency of each polymer was determined via ^{1}H NMR, which are presented in Appendix Figure 6.1.

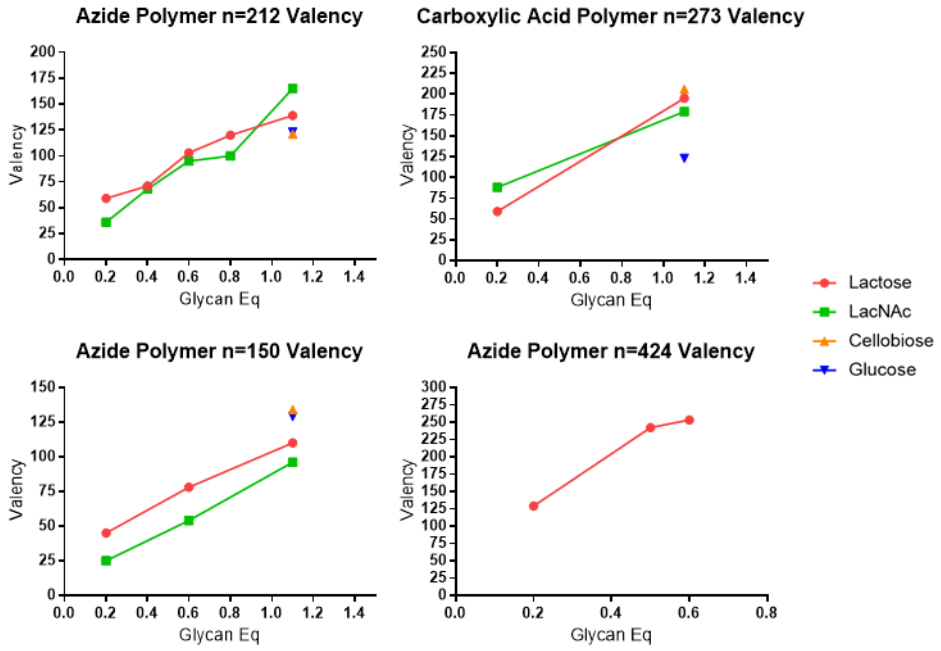

Figure 3.2: Glycan valency of each polymer. Valency was calculated by multiplying the polymer length by the sugar ligation efficiency. The sugar ligation efficiency was calculated by subtracting polymer backbone protons from the total integration of the region δ2.5-4.5 ppm and then dividing by the number of glycan protons. As cellobiose and glucose are serving as a control for lectin specificity, only one valency was generated. The valency of the cellobiose and glucose polymers were similar for each polymer.

After characterization of the TAMRA labeling and the valency, the n=212 polymers were printed onto a cyclooctyne-functionalized epoxysilane glass slide. The procedure, as well as the printing buffer, was adapted from previous lab printing methods. An image of the print is shown in Figure 3.3. The spot morphology appeared to decrease in uniformity as the concentration of polymer was reduced, as seen by the aggregation of polymer in the middle of the spot. Additionally, coffee rings are present, shown by the slight increase in fluorescence and consequently, polymer on the outside of the spot. Since uneven distribution of polymer and glycan organization can influence

lectin binding, printing buffer optimization was deemed necessary to produce uniform spots.

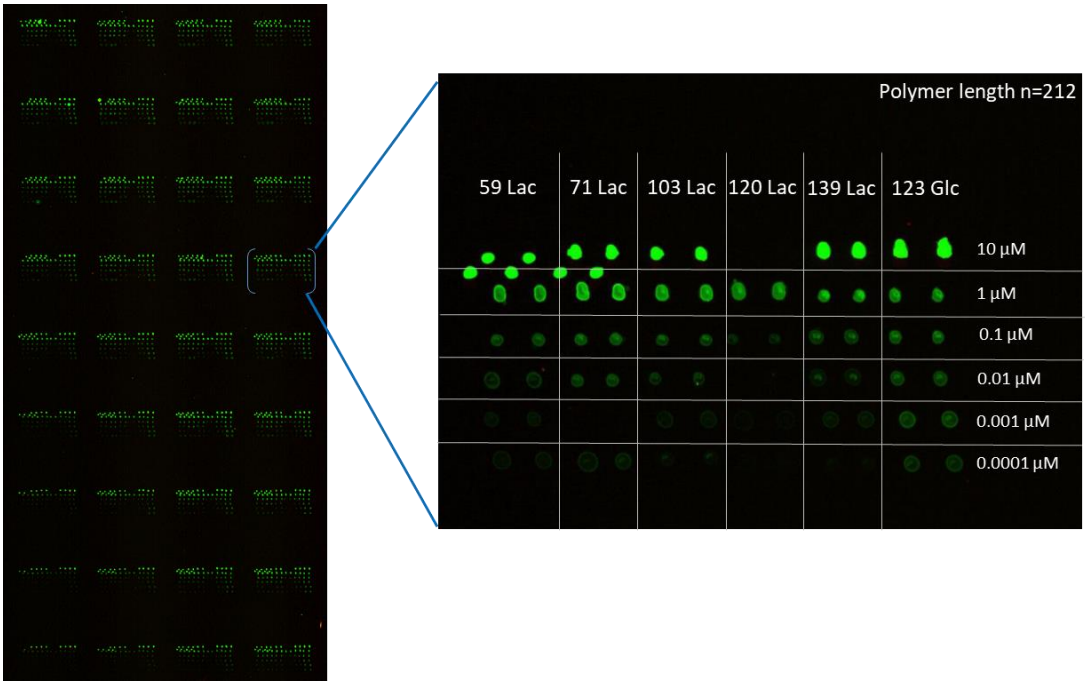

Figure 3.3: Initial microarray print of Azide n=212 polymer. The Azide n=212 polymer was printed on a cyclooctyne slide at a humidity of 75-80%. The full slide is shown on the left, whereas pictured on the right is an image of a representative array. The printing buffer consisted of 0.005% Tween-20 in 1X PBS. The four unaligned spots were made due to printer error.

Numerous printing buffers were tested obtain more uniform spot morphology. Glycerol was incorporated to increase hydrophilicity in an attempt to avoid the spot drying during printing. However, higher concentrations of glycerol had the negative effect of increasing spot diameter to larger than required sizes. Multiple concentrations of BSA were also tested to remove the coffee ring effect by competitively displacing the glycopolymers from the air/water interface.[39] Salts, such as betaine, were incorporated along with Tween-20 to prevent non-uniform drying of the spots. Spot morphologies obtained using various printing buffers are shown in Figure 3.4. Most printing buffers

tested were not ideal, either promoting non-uniform spot drying in the middle of the spot or at the air-water interface. The printing buffers containing betaine appear to have more even spot morphology as shown in Figure 3.4, and a buffer containing 1.5 M betaine, 0.05% glycerol, and 0.1% BSA was deemed the optimal printing buffer across a range of glycopolymer concentrations.

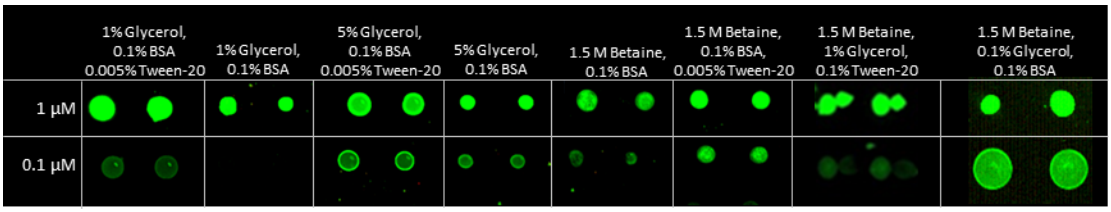

Figure 3.4: Printing buffers tested for optimal spot morphology. Each printing buffer was tested with 123 Glc n=212 polymer. Concentrations of 1 µM and 0.1 µM to determine the ideal printing buffer for uniform spot morphology and size.

With the printing buffer optimized to provide even spot morphology, full density variant arrays were printed. However, after comparing images of the arrays from pre-wash to post-wash, the spots appeared to move. This is even apparent in the initial test prints of the betaine solution containing 0.1% Tween-20 in Figure 3.4, in which the 1 µM and 0.1 µM solutions have a second spot that arises after the washing procedure. This is presumably due to two factors: the incomplete drying of spots in the presence of glycerol, and the relatively hydrophobic surface of the cyclooctyne-coated glass substrate. While the spots traveling did not occur for every print and for every array, it occurred frequently enough to impact the ability to analyze lectin binding, as the spots were no longer uniform.

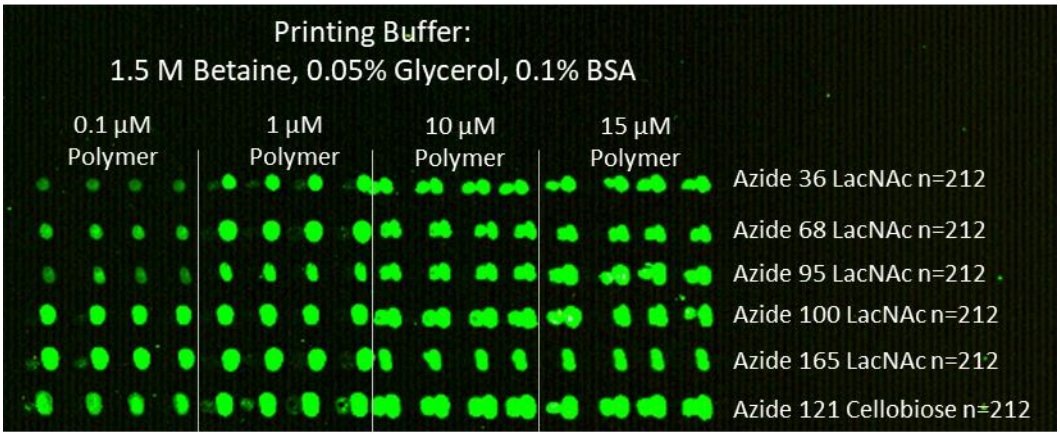

Figure 3.5: Printing buffer causing spot movement while washing. One example of an array in which the spots moved during the washing procedure. The movement of the spots appeared to be independent of the valency of the polymer, as well as of the glycan attached to the polymer, based on numerous slides.

The copper-free cyclooctyne "click" method of grafting the glycopolymers to the surface offers many advantages. The main benefit is not incorporating an extra reagent, such as a copper catalyst into the printing conditions. It is also arguably more biologically friendly than copper click, due to the lack of potentially toxic catalysts remaining on the array after washing. This immobilization method also removes the need to wash the slide with agents such as EDTA to remove the copper which could inhibit lectin binding if not properly removed. However, cyclooctyne attached to the substrate can make the slide surface more hydrophobic which can possibly affect polymer grafting, spot morphology, and retention, as seen in the betaine printing buffer. In an effort to generate array substrates more suitable for uniform spot printing, we turned to the copper click process, which offers a broader range of surface functionality with more tunable physical properties.

First, propargylamine was explored for polymer immobilization due to its increased hydrophilicity compared to cyclooctyne. The substrates were prepared by the

treatment of epoxysilane slides with propargylamine in the presence of DIPEA in DMF overnight. Four freshly functionalized slides, three propargylamine functionalized and one cyclooctyne functionalized, were printed consecutively with a LacNAc polymer (n = 212, valency 68) using the same 9 printing solutions throughout all four slides. In an attempt to determine the optimal reaction conditions for the copper-click reaction to occur numerous conditions were evaluated. Two propargylamine slides and the cyclooctyne slide were allowed to react overnight, with one propargylamine slide allowed to react at room temperature, and one propargylamine slide along with the cyclooctyne slide was allowed to react at 4°C, following established printing procedures. The final propargylamine slide was allowed to react at room temperature for two hours before washing. The fluorescent intensity for the multiple slide functionalizations are shown in Figure 3.6, below, and images of an array printed onto the cyclooctyne slide and a propargylamine slide are shown in Appendix 6.2.

Multiple printing buffers were used to optimize the printing conditions for the copper-click reaction. The different printing buffers contained the LacNac polymer (n = 212, valency 68, 0.1 μM, 1 μM, 10 μM) in solvent containing a Cu catalyst and either: NaCl to promote even spot morphology, TBTA to act as a Copper(I)-stabilizing ligand, and t-BuOH or DMSO to aid in solubilizing TBTA.[40] There was little difference in the fluorescent intensity between the propargylamine slide allowed to react for two hours and the propargylamine slide allowed to react overnight. Additionally, the different printing buffers had a slight effect on polymer grafting, with solution 8 containing 0.05% glycerol in addition to sodium ascorbate and copper (II) sulfate having the greatest fluorescent intensity on the first propargylamine slide.

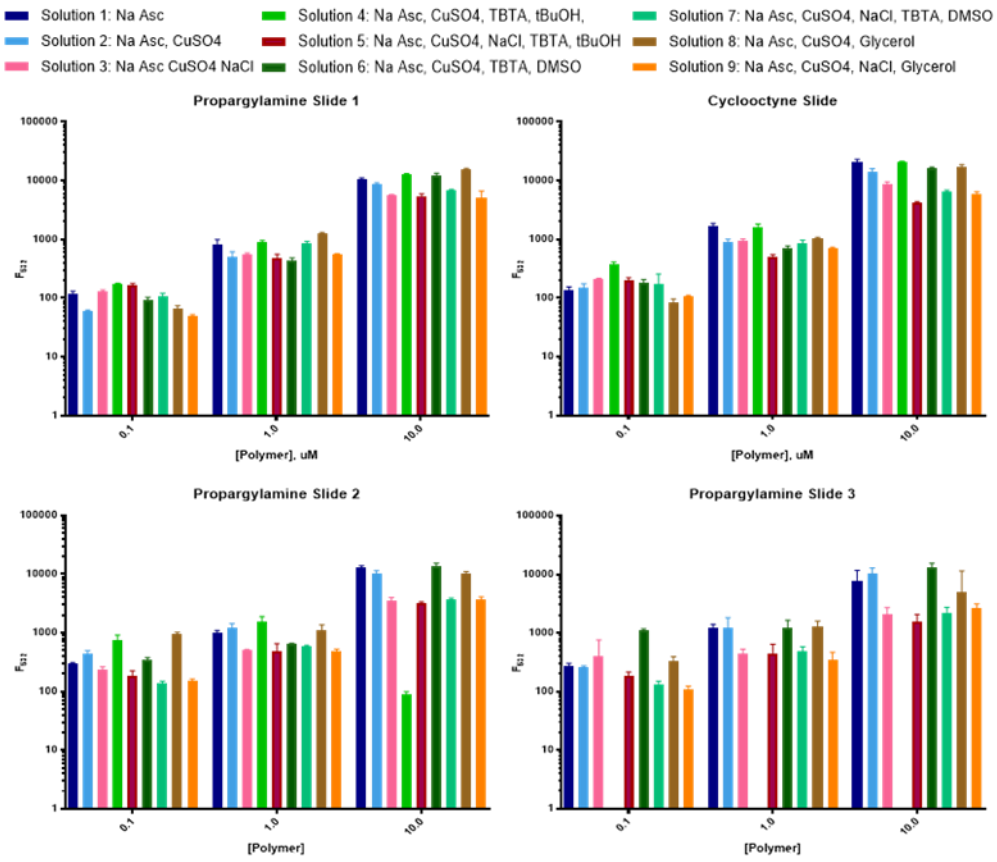

Figure 3.6: Comparison of glycopolymer grafting efficiency between propargylamine functionalized slides and a cyclooctyne functionalized slide. All printing solutions contained 0.1% BSA. Polymer fluorescence, F532, for each printing condition is shown on a log 10 scale. All four slides were scanned at a F532 PMT of 300. Propargylamine Slide 1 was allowed to react overnight at 4°C; Propargylamine Slide 2 was allowed to react for two hours at room temperature; Propargylamine Slide 3 was allowed to react overnight at room temperature; Cyclooctyne Slide was done under allowed to react overnight at 4°C, as per normal printing protocol. Solution 4 of the Propargylamine Slide 3 was not able to be analyzed due to printer error, and the spots of the10 μM Polymer solution for Propargylamine Slide 2 also did not print well, as seen in the appendix.

The most notable feature of the propargylamine arrays are that the first printing buffer, consisting of: sodium ascorbate, BSA, and PBS still showed fluorescence after vigorous washing in two 0.1% Triton-X/PBS solutions, even though no copper catalyst was added to the printing buffer. Due to the microarray printer used, trace amounts of

copper could have entered the wash solution used to rinse the tip between each printing solution and allow the click reaction to occur.

To verify these findings, a small print of the same polymer (LacNAc n = 212, Valency 68) was printed onto another propargylamine-functionalized epoxysilane slide which was functionalized with propargylamine immediately prior to printing. The polymer was printed in a 0.1% BSA PBS solution utilizing a new array tip on the microarray printer, to eliminate the possibility of copper entering the print. After printing and allowing to react over night at 4°C, the slide was initially washed with 0.1% Triton-X/PBS, and then imaged. At this step, retention of the polymers was still observed, suggesting that non-specific background binding of the polymers to the array substrate continued to occur.

Under the suspicion that electrostatic interactions could be contributing to the nonspecific polymer grafting, concentrated salt solutions were used for subsequent washes of the same slide. After the 0.1% Triton-X/PBS wash, the slide was then washed with a 1 M NaCl solution and imaged, and then again with a 1.5 M NaCl solution in 0.1% Triton-X/PBS. The fluorescent intensity immediately after printing and after each wash procedure is shown in Figure 3.7. The fluorescent intensity was reduced after the first wash, but showed little reduction in intensity following subsequent washing despite the lack of copper to catalyze the azide-alkyne click reaction.

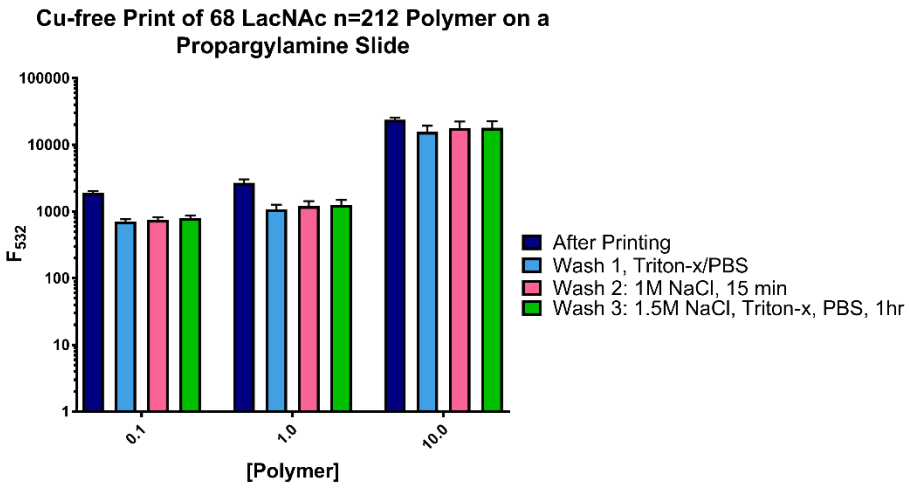

Figure 3.7: Polymer fluorescence after subsequent NaCl washing procedures. F_{532} is the fluorescent intensity. Wash 1 consisted of normal washing procedure: vigourous washing in 0.1% Triton-X/PBS, followed by rocking in 0.1% Triton-X/PBS solution before two washes in PBS before rinsing in Milli-Q water and spin-drying. Wash 2 consisted of rocking in 1 M NaCl in PBS for 15 minutes before rinsing in Milli-Q water. The final wash consisted of rocking in 1.5 M NaCl in PBS for an hour, followed by two washes in PBS for 10 minutes, before rinsing in Milli-Q water and spin-drying.

With increasing vigorousness of washing conditions failing to eliminate background binding of polymers, different surface passivation strategies were explored. All previous prints up to this point were passivated in a 1% BSA solution for an hour immediately prior to printing. BSA is a blocking agent commonly used to reduce nonspecific binding by forming a molecular layer of BSA on the slide.[41] While the BSA passivation should be adequate based on literature precedence, it is possible that it does not coat the surface effectively enough to cover any unfunctionalized epoxide groups on the slide. This could allow the glycopolymer to bind to the surface via the unreacted aminooxy groups on the polymer side-chains.

Ethanolamine has previously been used to open residual epoxide groups left on the surface, capping them with hydroxyl groups.[42] Two slides, one cyclooctyne-

functionalized and one propargylamine-functionalized, were passivated in an ethanolamine/tetraborate buffer for 3 hours before passivation in 1% BSA. To ascertain what effect, if any, the ethanolamine passivation has on polymer grafting, one cyclooctyne slide and one propargylamine slide were passivated following the normal protocol, 1% BSA for one hour. Carboxylic acid-terminated polymers were obtained, fluorophore labeled, and ligated with sugar to measure the amount of nonspecific binding of the polymer to the surface. Additionally, EDTA solutions were employed on both propargylamine slides, and were printed separate from the copper containing printing buffer. The polymer fluorescence data are shown in Figure 3.8. Both carboxylic acid polymers, ligated with either Lactose or LacNAc, along with the azide-terminated polymers printed in an EDTA printing buffer, are still present under all passivation conditions despite vigorously washing the slide with 0.1% Triton-X/PBS.

Interestingly, the polymers containing LacNAc show a higher fluorescent intensity. The exception is the carboxylic acid-terminated polymer 179 LacNAc, n=273, on the 1% BSA (referred to as “Normal”) passivated propargylamine slide, which was not printed due to pin malfunction. These LacNAc-containing polymers could have increased hydrophobicity due to the acetamido group present on LacNAc. While the slides are commercially bought with an Epoxysilane coating, it is possible that the aminooxy group present on unligated polymer side-chains is interacting with the surface.

Collectively, the printing experiments on both cyclooctyne and propargyl amine functionalized epoxy slides show significant background binding of all polymers, which is more pronounced for the more hydrophobic LacNAc glycans. The observed

background binding may be caused by the surface functionalization chemistry, hydrophobicity of the polymers or electrostatic interactions between the protonated unreacted aminooxy polymer sidechains and the array surface. The epoxy substrates, which are obtained from a commercial source, may have additional proprietary surface modifications, further complicating analysis. Therefore, additional surface chemistries were evaluated.

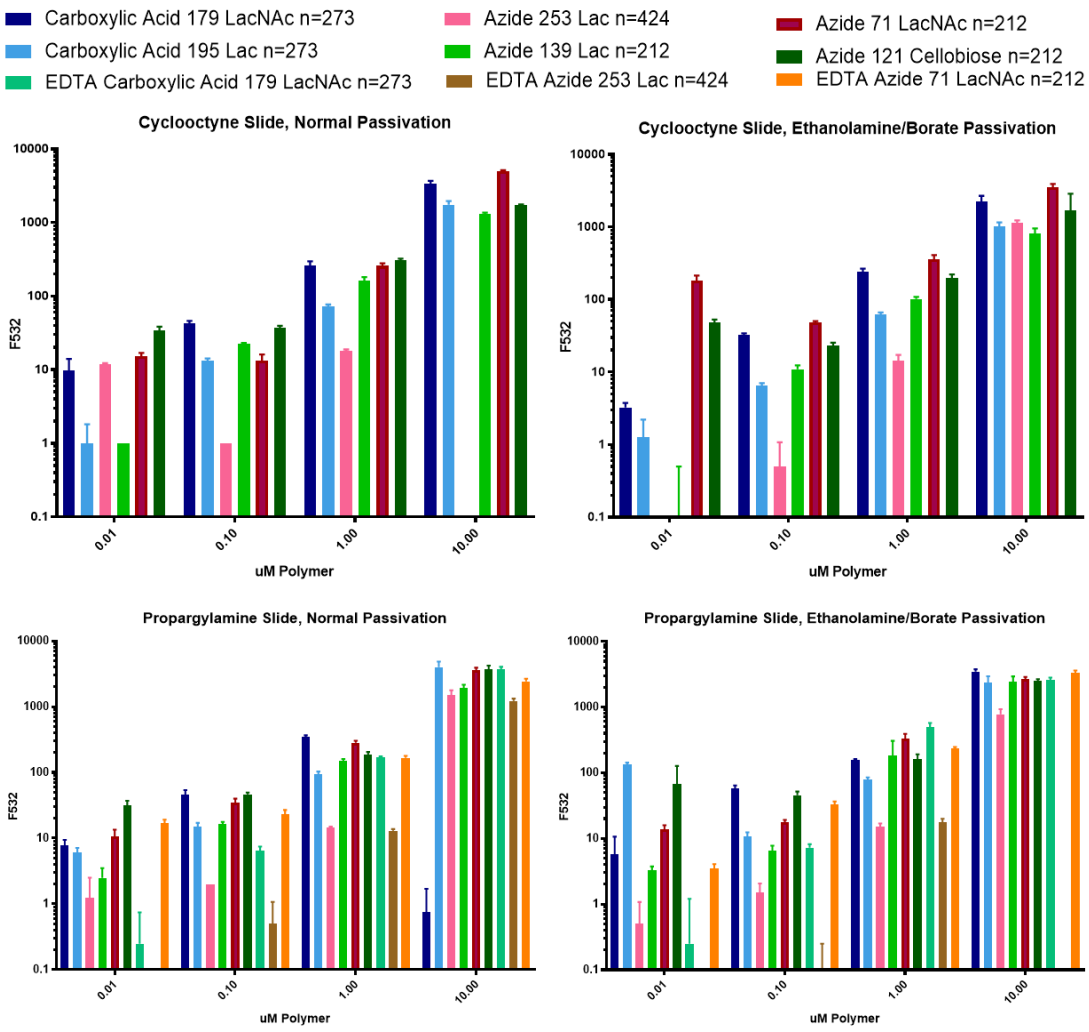

Figure 3.8: Evaluation of ethanolamine passivation on propargylamine and cyclooctyne slides. F_{532} is the fluorescent intensity. Despite passivating in an ethanolamine/tetraborate buffer prior to 0.1% BSA passivation, nonspecific attachment of polymer to the slide was still present. Normal passivation method includes rocking in a 0.1% BSA/PBS solution for an hour, prior to rocking in Milli-Q water for 15 minutes, 3x.

To generate a more controlled hydrophilic surface, which should be resistant to non-specific glycopolymer binding, the epoxysilane slides were functionalized with diamino poly(ethylene glycol) (dPEG) under marginal solvation conditions, referred to as cloud point, due to the reduced interchain repulsion of PEGs at increased temperature.[37] Previous work has been done on utilizing dPEG as a passivation method to generate non-

fouling extracellular matrix protein microarrays.[43] Extra-cellular matrix proteins were contact printed onto epoxy slides, enabling cell capture after seeding, the slides were then passivated with either dPEG or BSA to resist cell attachment and nonspecific protein adsorption.[43] In that study, based on the amount of cell attachment, it was determined that the optimal dPEG passivation occurred using 10,000 Da dPEG, and provided effective passivation for a longer period compared to BSA passivation.

The functionalization of epoxysilane slides with diamino-PEG, along with BSA passivation, could reduce nonspecific binding of the glycopolymers by generating a non-sticky surface via PEGs inertness and hydrophilicity. Fresh epoxysilane slides were functionalized with 10 KDa dPEG under cloudpoint conditions at 65°C, overnight. Following the dPEG functionalization, propargylic acid was attached to the amine via EDC coupling. The reaction scheme for these reactions is shown in Figure 3.9.

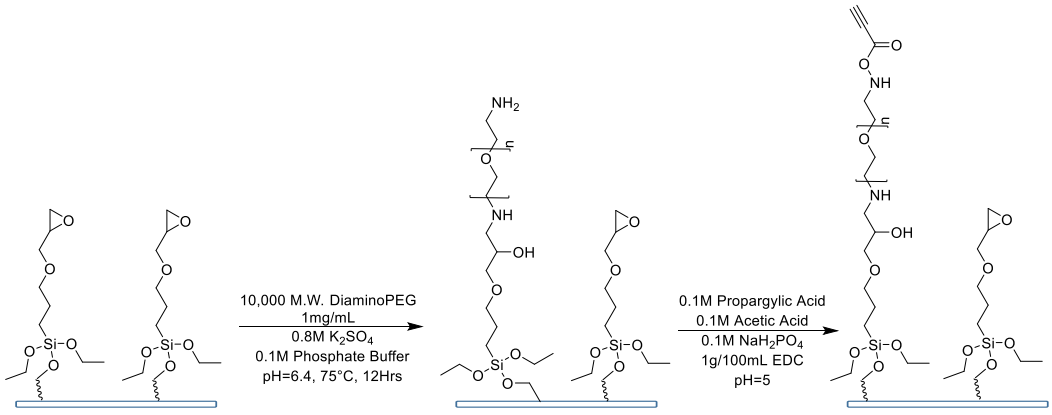

Figure 3.9: Schematic of the dPEG functionalization and subsequent EDC coupling reaction with propargylic acid. Epoxysilane Superchip slides were placed in a 1mg/mL dPEG solution at cloudpoint for 12 hours. The slides were then placed in a 0.1 M propargylic acid solution to couple the propargyl to the remaining amine.

Contact angle measurements were taken for dPEG functionalized slides and propargylic acid functionalized slides and compared to unfunctionalized epoxysilane slides as well as cyclooctyne slides over a period of 4 days (Figure 3.10). The dPEG slides showed reduced contact angles (34.7° ± 3.1, day of functionalization) compared to the epoxysilane slide (51.0° ± 1.7, day of functionalization), indicating increased hydrophilicity and providing some evidence that the dPEG cloudpoint functionalization is altering the surface of the slide. However, as shown in Appendix Figure 6.2, there is a gradient present on the diaminoPEG slides. Additionally, the differences in contact angle between the epoxysilane slide and the dPEG slide, as well as between the dPEG slide and the dPEG-Propargyl slide (45.6° ± 5.0, day of functionalization) indicates a change occurred on the surface of the slide, although it does not fully prove the introduction of reactive alkyne functionality.

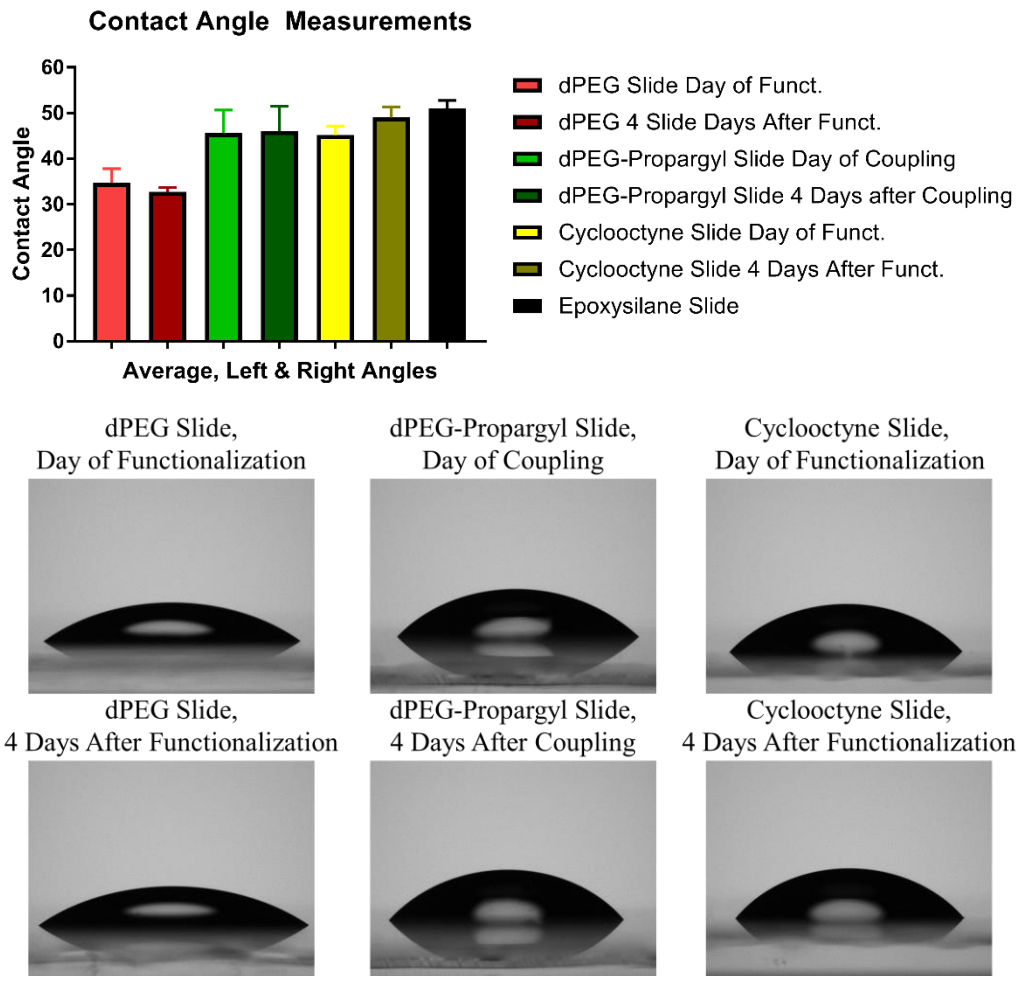

Figure 3.10: Characterization of array substrate surfaces using contact angle measurements. Contact angle measurements taken are averages of 50 angle measurements taken from three drops of deionized water on the top, middle, and bottom of the slides.

Another method to evaluate the effectiveness of the dPEG functionalization was by reacting the resulting amine surfaces with NHS-Ester AF647. Epoxysilane slides were partially functionalized with diaminoPEG. Following this, covalent immobilization of AF647 via amide bond formation was assessed by titrating amino-PEG functionalized slides with increasing concentrations of AF647. Figure 3.11 shows the results of this test, in which only the highest concentration showed a meaningful fluorescent signal. The

unfunctionalized side had no observed fluorescence present, indicating the fluorescent signal seen is due to the fluorophore attaching to the amino groups present on the slide. This method was later used to evaluate the effects of increasing the amount of blocking agent used, which is shown in the Appendix Figure 6.3.

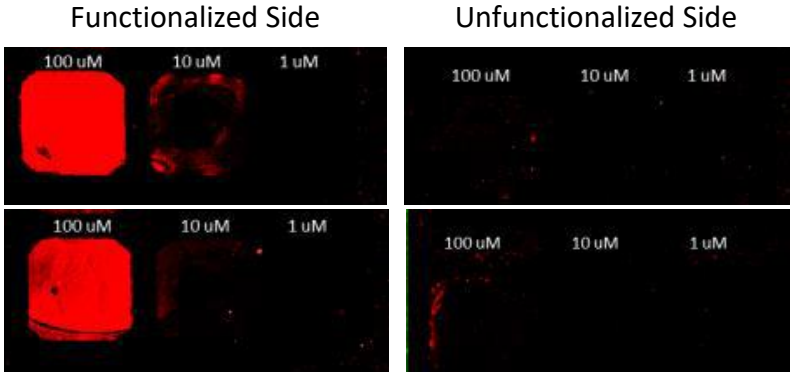

Figure 3.11: NHS-Ester AF647 applied onto a partially functionalized dPEG slide. The slide was functionalized in a coplin jar filled halfway with the cloudpoint dPEG solution. NHS-Ester AF647 was applied in a HEPES buffer and allowed to react for four hours prior to washing in HEPES buffer.

Knowing that the propargylic acid coupling was altering the surface of the slide, azide and carboxylic acid polymers were printed on a dPEG-Propargyl slide and a cyclooctyne slide, both passivated with 1% BSA, to determine if the non-specific binding is still present on the altered surface. The glycopolymers tested and their fluorescence is shown in Figure 3.12. While the nonspecific binding of the polymers to the propargyl-PEG surfaces was not fully eliminated, there was a decrease in fluorescent intensity of printed polymer spots on this surface compared to the cyclooctyne-coated slide. To evaluate if the glycans themselves were sticky, a polymer ligated with 6’ sialyllactose, a negatively charged glycan consisting of an acetylneuraminic acid unit connected to the 6 position of the galactose unit of lactose, was printed. The 6’ sialyllactose polymer consistently showed a lower fluorescent intensity compared to the uncharged lactose or

LacNAc polymers, but still exhibited nonspecific grafting when printed in the absence of copper. Based on the continued presence of carboxylic acid polymers, as well as azide polymers printed in the absence of copper, it is clear the dPEG functionalization and BSA passivation are not effective at preventing nonspecific grafting of the polymer.

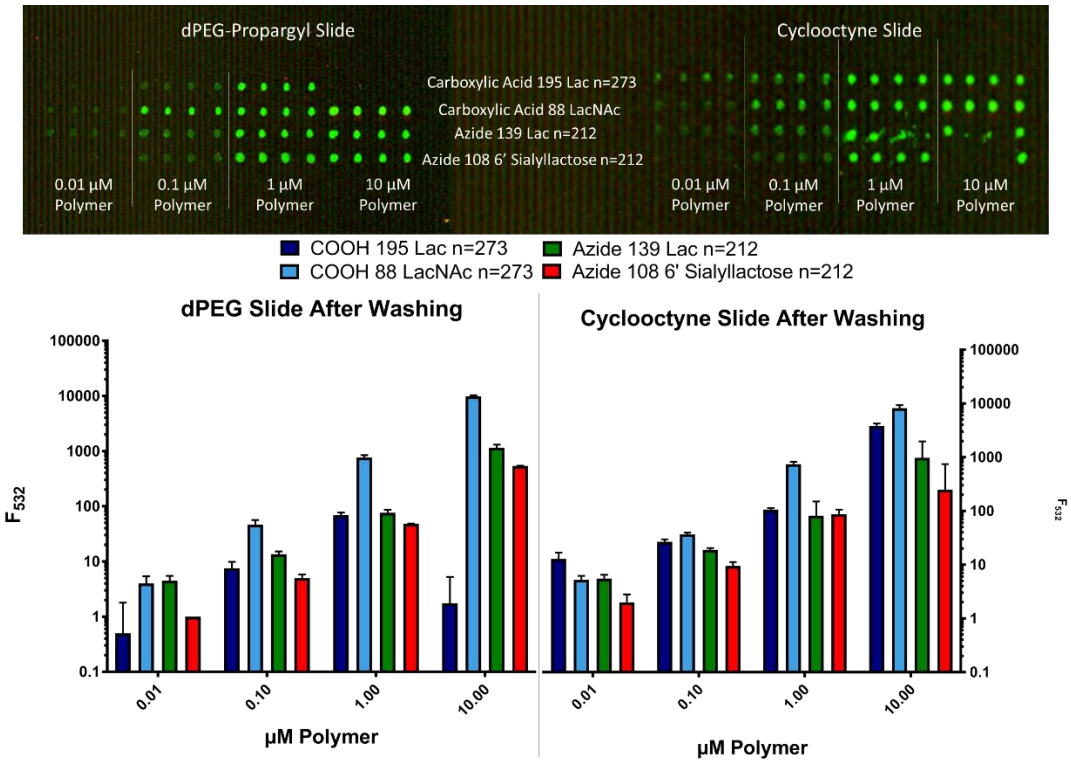

Figure 3.12: Comparison of dPEG-Propargyl functionalized slide to Cyclooctyne functionalized slide. F_{532} is the fluorescent intensity. To evaluate the effectiveness of diaminoPEG-Propargyl slides at reducing nonspecific grafting of the polymer, a cyclooctyne slide was printed with a dPEG-Propargyl slide using the same printing solutions.

Casein, a family of milk proteins, have previously been used as a blocker to reduce non-specific adsorption of proteins.[44] Casein could be a more effective blocker due to containing a broad range of molecules of different sizes and increased hydrophobicity. A 1% Casein solution in PBS was used as a passivation buffer on a dPEG-Propargyl slide which was printed alongside a dPEG-Propargyl slide passivated in

1% BSA. Neither passivation condition prevented the nonspecific grafting of the carboxylic acid or azide-terminated polymers printed in the absence of a copper catalyst. Additionally, TAMRA with a carboxylic acid linker attached was printed on both slides, and was still present after washing. The fluorescent intensities for each condition is shown in Figure 3.13 below, and images of each are shown in the Appendix Figure 6.4. Finally, the amount of fluorescence lost from washing is shown in Appendix Figure 6.6, in which the glycopolymers printed in the absence of a Cu-catalyst showed a small increase in fluorescence lost.

After normal washing conditions, the slides were also vigorously washed in a PBS solution (pH = 10) for 2 minutes, followed by rocking in a new PBS solution, which was repeated 3x. This was followed by the same procedure repeated in a saturated NaCl solution. The basic wash was performed to remove electrostatic interactions by deprotonating the N-methylhydroxyamine on the polymer side chains not ligated with glycans. The fluorescence decreased slightly after the basic wash, and did not change after the saturated NaCl wash, showing nonspecific binding was present for both conditions, as shown in Appendix Figure 6.5.

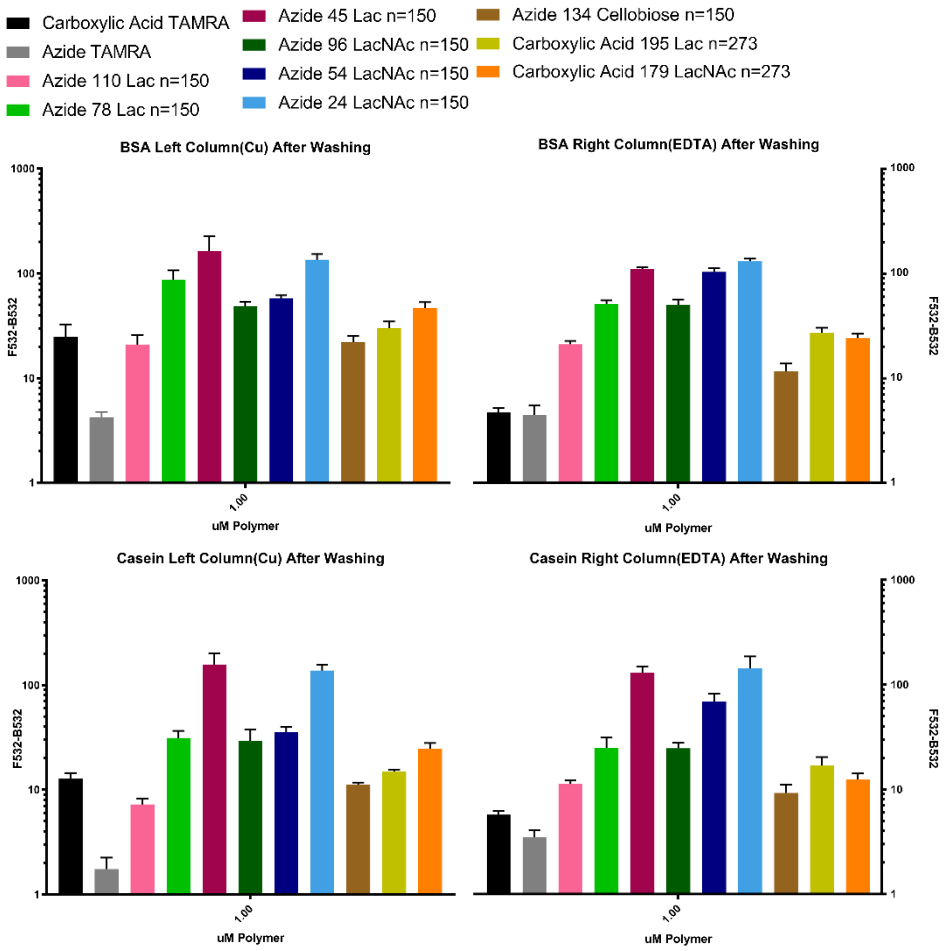

Figure 3.13: Evaluation of Casein passivation in comparison to BSA passivation. Each dPEG-Propargyl slide was passivated for an hour in 1% of each respective blocking agent. Neither passivation method appears effective at preventing the nonspecific grafting of the glycopolymer

Nonspecific binding of the glycopolymers is evident despite numerous different slide functionalizations and passivation methods. The epoxysilane Superchip brand of slides could be unsuitable for use with the current glycopolymer. As a final test, commercially-prepared high-density alkyne slides were purchased from MicroSurfaces, Inc. The slides consist of terminal alkyne groups attached to a PEG coating.

A print was conducted on one MicroSurfaces high-density alkyne slides alongside two dPEG-Propargyl functionalized Thermo Fisher slides. Glycopolymers were arrayed on the MicroSurfaces slide and one of the dPEG-Propargyl slides following the printing protocol supplied by MicroSurfaces, whereas the remaining dPEG-Propargyl slide was printed following the previously established protocol protocol (1% BSA Passivation, 1 Hour). The printing buffer was made according the supplied protocol, and included 10% gycerol, which resulted in poor spot morphology on both dPEG-Propargyl slides. The printed slides were allowed to react for an hour before rocking in 1% Triton-X/PBS 3x for 15 minutes, per the supplied protocol. The MicroSurfaces protocol lacked a passivation method prior to printing, as the PEG coating should be sufficient to minimize non-specific binding. After the slide was washed an azide-linked small molecule blocker was applied. The results of the MicroSurfaces print are shown below in Figure 3.14

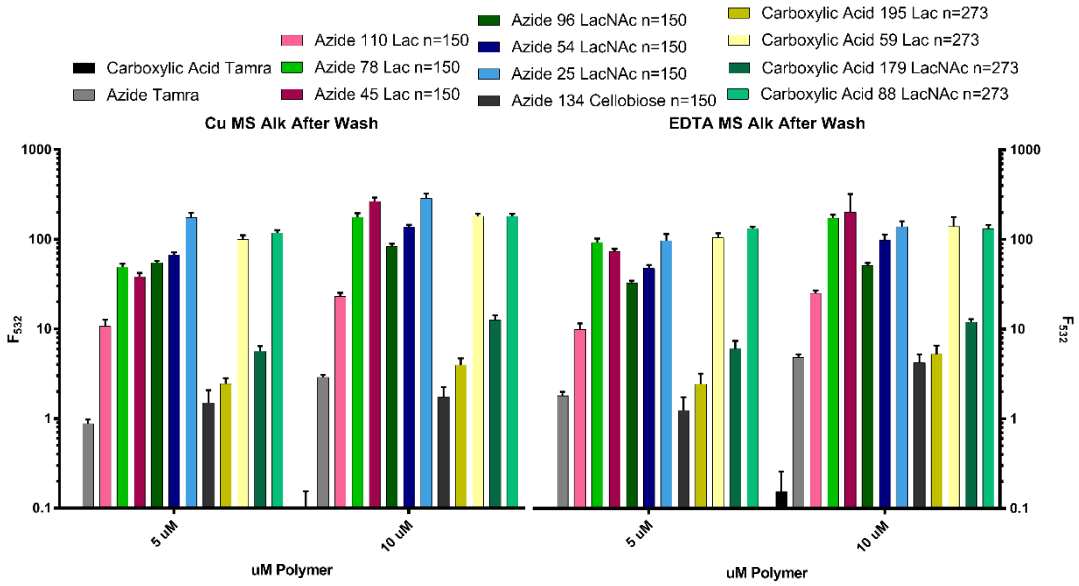

Figure 3.14: Evaluation of a commercially obtained high-density alkyne slide. Polymers and TAMRA were printed per the MicroSurfaces, Inc. protocol supplied at a humidity of 65%. The printing buffer consisted of 10% Glycerol, 0.3 μM $CuSO_4$, 2 μM Ascorbic Acid, 0.3 μM Bathophenanthroline, and 1x PBS. The printed slide was allowed to react in a humidified chamber for 90 minutes before rocking in 0.1% Triton-X/PBS for 15 minutes, 3x, followed by rinsing in Milli-Q water, spin-drying, and imaging. Values shown are normalized to TAMRA, due to differing fluorophore-labeling efficiencies of the various glycopolymers.

Based on the results of the MicroSurfaces slide print, the small molecule carboxylic acid TAMRA does not seem to stick to the high-density alkyne, as shown in images of the arrays (Appendix Figure 6.7). This could be due to residual copper entering that solution throughout the print. The lack of nonspecific binding of the carboxylic acid TAMRA provides further evidence that the carboxylic acid polymers remaining on the slide is likely due to the structure of the polymer itself. It should be noted that the glycopolymer was printed from 0.1 μM to 10 μM per polymer, and there should be much less azide present in the glycopolymer solutions than in the azide TAMRA solutions of the same concentration of TAMRA. Furthermore, the lower valency polymers have a higher fluorescence intensity, likely due to the removal of steric effects caused by the sugars. Additionally, the side-chains without sugars have a greater amount aminooxy

groups, as well as secondary amines, which could be contributing to the unspecific grafting, accounting for the increase in fluorescence seen in the lowest valency polymers.

The small molecule azide TAMRA shows fluorescence in both the printing solutions containing a Cu catalyst, and the printing solution lacking one. However, when looking at the total amount of fluorescence lost after washing (Figure 3.15), the azide TAMRA printed in the absence of a Cu catalyst loses the most fluorescence, even more than the carboxylic acid TAMRA, and much more than when printed in the presence of a Cu catalyst. The lower valency glycopolymers do exhibit lower fluorescence lost than the higher valency glycopolymers, coinciding with the overall higher fluorescence seen after washing. This provides some evidence that the aminooxy groups present on unligated side-chains are contributing to the non-specific binding of the glycopolymers.

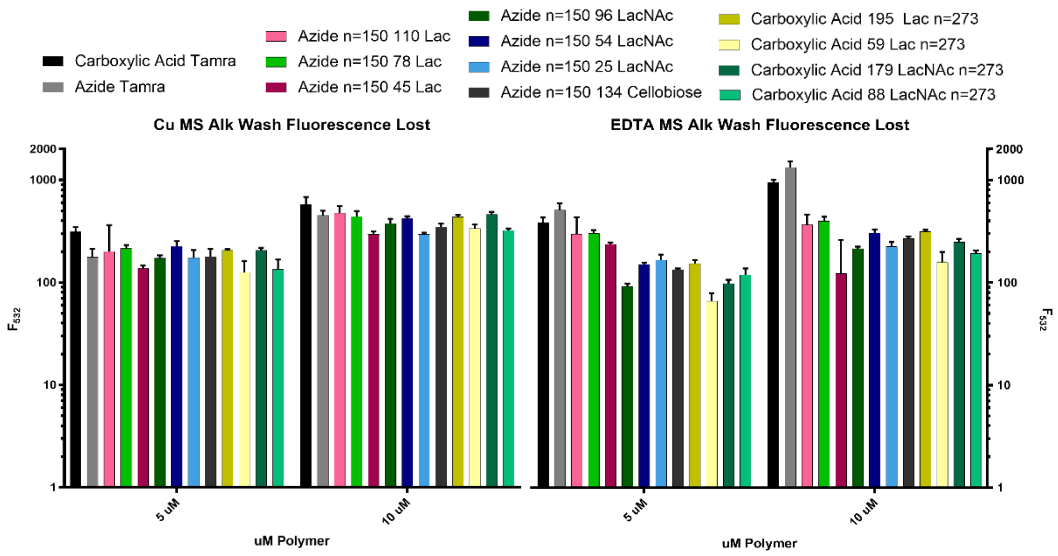

Figure 3.15: Evaluation of fluorescence lost on a commercially obtained high-density alkyne slide. Fluorescence prior to washing was subtracted by the fluorescence remaining after washing to determine the amount of fluorescence lost for each condition printed on the commercial high-density alkyne slide.

Due to the nonspecific grafting of the glycopolymers to the surface of the slides, the polymer and glycan presentation remains unknown, but is unlikely to be optimal. When hydrated, some of polymers could still be laying down on the surface of the slide due to stickiness of the aminooxy group, still allowing them to present their glycans for binding but in an uncontrolled manner. Other polymers in the same spot could be properly presented when hydrated, and could test for the multivalent binding interactions, such as crosslinking, of lectins. However, the uncontrolled presentation of some of the polymers would make it difficult to accurately parse out the most ideal glycan presentation needed for the crosslinking effects to occur. While the current array architecture can be effective for evaluating lectin binding specificity, is not suitable for the evaluation of multivalency and crosslinking in lectins with any reasonable accuracy. A potential solution to this problem, which remains to be explored, may be the redesign

of the polymer backbone to reduce the hydrophobicity, remove the unreacted aminooxy side-chains, and optimize conditions to better preserve the azide end groups.

The current array can still be used to determine the binding of lectins to different glycans. Many lectins, such as RCA_{120}, *Arachis hypogaea* (PNA), and MAL-I among others have specificities for certain glycans, but can tolerate substitutions. As an example, PNA preferentially binds the T-antigen, Galβ1-3GalNAc, but will also bind to Lactose as well as LacNAc.[46] RCA_{120} is a tetramer of two α-chains and two β-chains, and has a preference for terminal β-galactose residues, especially those connected to the underlying residues through a β(1,4)-linkage. The specificity for terminal β-galactose residues allows it to bind to multiple glycans, such as lactose and LacNAc. To evaluate the specificity and avidity of RCA_{120} in the density-variant microarrays generated binding assays were performed on glycopolymer arrays printed onto dPEG-Propargyl slides. Binding to the arrayed glycopolymers was performed over a range of RCA_{120} concentrations, and binding isotherms were constructed to extract apparent K_D values to the immobilized ligands, shown in Figure 3.15. The data points in the binding isotherms correspond to an average of 4 individual spots. Additionally, tables displaying the apparent K_D values, as well as the standard error and R^2 values are displayed in Table 3.2. Replicate binding curves and K_D performed on separate microarrays are presented in Appendix Figure 6.8. It should be noted that, due to the broad range of glycopolymer valency and of glycan density in a single array, not all conditions were able to reach saturation, limiting the ability to efficiently determine apparent K_D, but still provides information on the specificity of RCA_{120}.

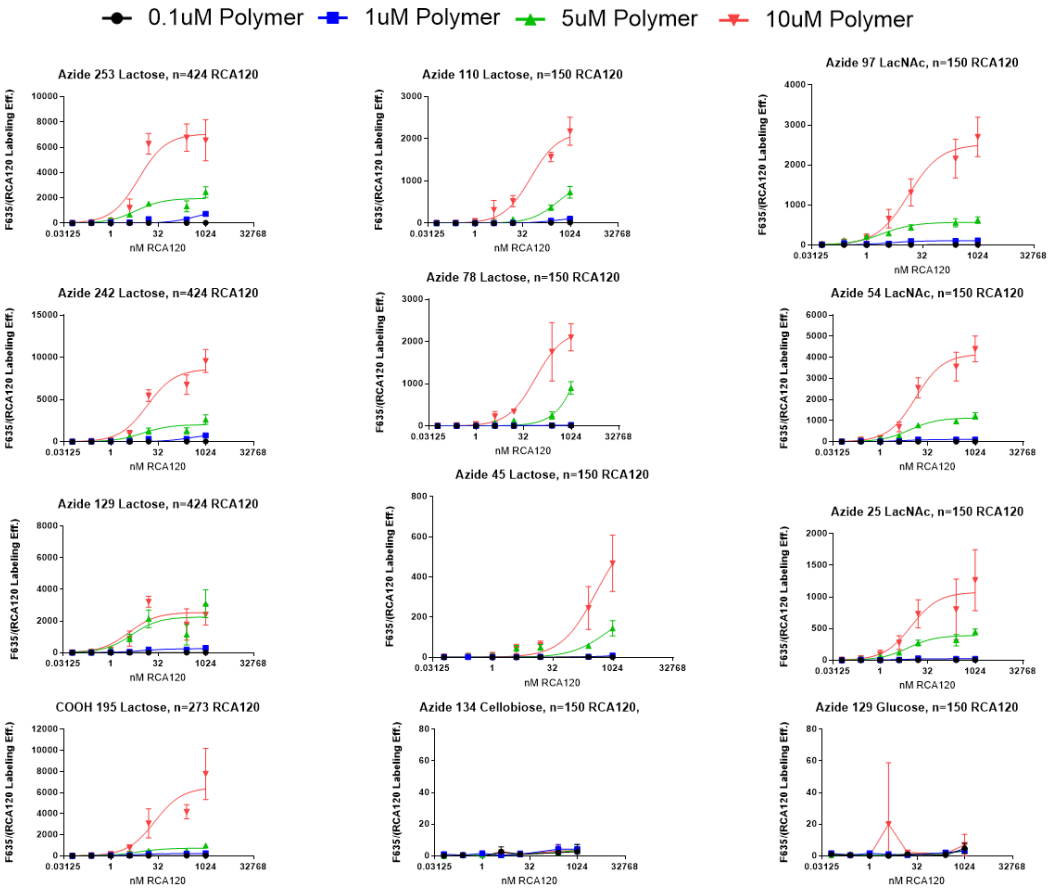

Figure 3.16: Binding curves of RCA_{120}. RCA_{120} was incubated for 1 hour at varying concentrations on separate sub-arrays printed onto the same dPEG-Propargyl slide. No apparent binding was observed for cellobiose or glucose, as shown by the scale of the curves generated. Based on some curves reaching saturation, such as the 253 Lac n=424 polymer at 10 μM, compared to the 45 Lac n=150 polymer, preferential glycan amount and spacing can be determined for the glycopolymer.

Table 3.2: Apparent K_D values of RCA_{120} with Lac and LacNAc glycopolymers. Binding curves with R^2 values above 0.9000 are italicized for emphasis. Under most conditions, such as the LacNAc glycopolymers as well as the Lac n=424 polymers, RCA_{120} appears to prefer the 5 μM glycopolymer concentration, likely due to optimal spacing between the glycopolymers on the surface.

Azide 253 Lac, n=424

[Glycopolymer]	Apparent K_D	Std. Error	R^2
10 μM	7.593	2.097	0.8841
5 μM	6.123	2.061	0.8163
1 μM	533.9	306.5	0.7561
0.1 μM	5.117	2.196	0.7089

Azide 110 Lac n=150

[Glycopolymer]	Apparent K_D	Std. Error	R^2
10 μM	*57.22*	*14.48*	*0.9498*
5 μM	*425.6*	*108.5*	*0.9525*
1 μM	*392.8*	*54.65*	*0.9851*
0.1 μM	322.8	129.3	0.8825

Azide 96 LacNAc n=150

[Glycopolymer]	Apparent K_D	Std. Error	R^2
10 μM	*13.42*	*2.998*	*0.918*
5 μM	2.618	0.619	0.872
1 μM	3.841	1.283	0.7237
0.1 μM	3.442	1.207	0.7495

Azide 242 Lac, n=424

[Glycopolymer]	Apparent K_D	Std. Error	R^2
10 μM	*14.15*	*3.338*	*0.9176*
5 μM	10.05	3.888	0.7753
1 μM	337.6	199.4	0.7169
0.1 μM	5.09	1.865	0.7758

Azide 78 Lac n=150

[Glycopolymer]	Apparent K_D	Std. Error	R^2
10 μM	*74.59*	*27.96*	*0.9112*
5 μM	*4447*	*5400*	*0.9353*
1 μM	19.81	8.854	0.7257
0.1 μM	-136.7	74.63	0.2543

Azide 54 LacNAc n=150

[Glycopolymer]	Apparent K_D	Std. Error	R^2
10 μM	*12.84*	*2.476*	*0.9405*
5 μM	*8.447*	*1.418*	*0.9458*
1 μM	4.697	1.751	0.7461
0.1 μM	3.103	1.425	0.6702

Azide 129 Lac, n=424

[Glycopolymer]	Apparent K_D	Std. Error	R^2
10 μM	6.483	4.278	0.5642
5 μM	4.538	2.442	0.6443
1 μM	*8.855*	*2.103*	*0.904*
0.1 μM	3.341	1.339	0.7403

Azide 45 Lac, n=150

[Glycopolymer]	Apparent K_D	Std. Error	R^2
10 μM	380.3	162.7	0.8716
5 μM	645.7	477.5	0.6424
1 μM	1746	3151	0.4303
0.1 μM	12.38	19.16	0.2435

Azide 24 LacNAc n=150

[Glycopolymer]	Apparent K_D	Std. Error	R^2
10 μM	9.377	4.272	0.7226
5 μM	7.473	1.777	0.896
1 μM	3.847	1.686	0.6906
0.1 μM	5.99	3.662	0.5248

Carboxylic Acid 195 Lac n=273

[Glycopolymer]	Apparent K_D	Std. Error	R^2
10 μM	24.22	10.41	0.7969
5 μM	7.109	2.568	0.7808
1 μM	6.436	1.455	0.8972
0.1 μM	4.633	1.646	0.779

One of the advantages of using our fluorophore-labeled glycopolymers is the ability to determine the relative amount of polymer, and therefore glycan, presented on the surface. This can be plotted in heat map form and used to provide a more comprehensive picture on the binding affinities of lectins in response to changes in glycan density on the surface. For example, a heat map of an array used for an RCA_{120} assay is displayed in Figure 3.16 below, with the determined K_D in nM displayed on top of each cell, where applicable. Predictably, RCA_{120} shows reduced binding as the glycan density of the polymer is decreased. However, RCA_{120} consistently has a lower K_D at 5 μM than at 10 μM for the LacNAc glycopolymers throughout all binding assays performed. This indicated that the higher glycopolymer concentration is likely too dense

for RCA_{120} to effectively diffuse throughout the spot. Interestingly, RCA_{120} appeared to prefer LacNAc glycopolymers over Lac glycopolymers at similar glycan densities. Finally, RCA_{120} showed little binding to both glucose and cellobiose, which possesses a terminal glucose.

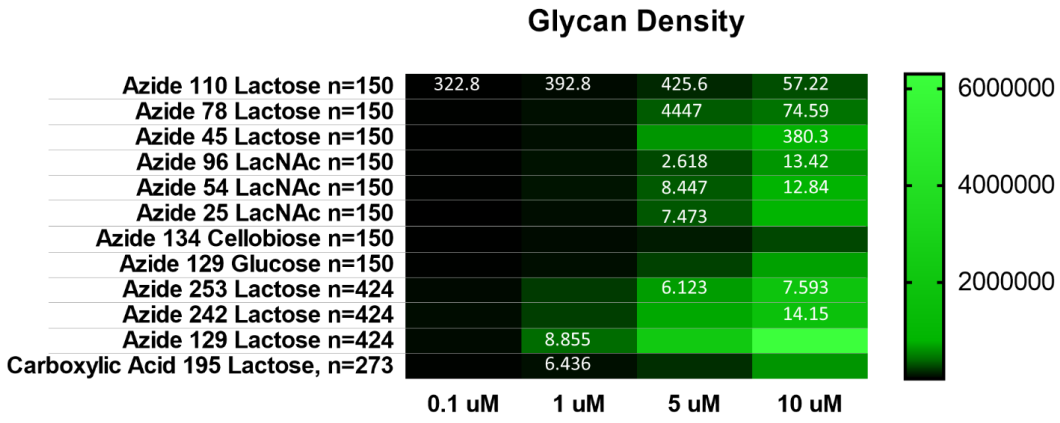

Figure 3.17: The distribution of glycan in an array. The orientation of the heat map is the same as an image of the array itself. Overlaid on certain cells are the determined K_D of RCA_{120}. The values used are obtained from binding curves where the R^2 value is greater than 0.90.

IV. Conclusion

Glycans, as well as glycan-binding proteins, are becoming an intensely studied subject in recent years. They play a myriad of important roles throughout an organism's life cycle, but due to their nontemplated synthesis and the structural heterogeneity of the glycome the study of individual lectin-glycan interactions can be a daunting task. Numerous methods to study these interactions have been developed, but many are resource- and time-intensive. The need for a high-through-put method of analyzing and determining the multivalency of lectins is exists.

In this work, a density-variant glycan microarray has been developed for the high-throughput determination of lectin binding characteristics. Glycopolymers of varying lengths and glycan valencies were printed at a range of concentrations. Varying the length and valency of the polymer may allow for the study of the ideal glycan spacing necessary for optimal lectin binding and the identification of distinct multivalent binding modes and crosslinking. Additionally, by printing the glycopolymers at a range of concentrations, the ideal spacing between glycans within individual polymers, as well as of proximal polymer chains, can be studied.

While the glycopolymer used has many advantages, such as its similarity to native mucins as well as unmodified sugars to be directy ligated to the side-chains, the current structure is limiting the potential of the microarrays. The orientation and attachment of the polymer on the surface remains unknown, due to the significant nonspecific binding of the polymer to the surface. A series of experiments aimed at determining the nature of

this non-specific binding revealed that nonspecific binding is generally greater for glycopolymers of lower valency, indicating the aminooxy present on residual unmodified side-chains may be the reason for the nonspecific grafting. Additionally, LacNAc glycopolymers are more likely to nonspecifically bind to the surface, likely due to the underlying N-actylglucosamine residue. Finally, because there is little difference in binding to the surface between glycopolymers terminated with a carboxylic acid and azide glycopolymers, it is likely that the terminal azide group is degraded during the glycopolymer synthesis. This is further supported by the IR data taken in the laboratory shown in Appendix Figure 6.9, in which the threshold needed to be lowered in order to see an azide peak on an azide terminated n=22 polymer. These factors makes the current microarray method unsuitable for the detailed analysis of lectin binding modes and evaluation of the lectin's crosslinking ability. Despite this, it is still an effective tool for evaluating lectin binding specificities.

To reach the full potential of these density variant glycan arrays, the structure of the polymer must be altered. One possible method may be generating copolymers of our current monomer and (2-oxopropyl)acrylate. Unmodified glycans could still be ligated to the acrylamide polymer side-chains, with the valency controlled by the amount of (2-oxopropyl)acrylate introduced to the original copolymer. The addition of a neutral monomer would decrease the amount of free aminooxy groups remaining on the polymer, potentially reducing the nonspecific grafting while providing a similar overall structure as the current backbone. Polymers of (2-oxopropyl)acrylate with a reactive alkyne group have also been shown to wash away on azide-functionalized chips when printed in the absence of a copper catalyst.[32] Utilizing terminal alkyne groups on the proposed

copolymer would also address the issue of the azide degradation throughout the glycopolymer synthesis, although it would remove the ability to utilize Cu-free click chemistry.

The density-variant glycan microarray presented in this work shows much promise as a method for screening lectin specificity, as well as probing multivalent interactions. Aside from presenting the carbohydrates in a more natural manner than typical glycan microarrays, the fluorophore on the glycopolymer allows for the determination of relative glycan present on the surface, providing further context for the different lectin specificity seen on binding assays.

Based on the three RCA_{120} binding assays presented, the apparent K_D may differ between each array, but the overall binding trend remains similar. RCA_{120} appears to favor the less dense 5 μM over the 10 μM condition, likely due to a more favorable polymer density on the surface. RCA_{120} also appears to prefer LacNAc glycopolymers over Lac glycopolymers printed under similar conditions.

V. References

1. Varki, A., and N. Sharon. "Historical Background and Overview." *Essential of Glycobiology*. Eds. A. Varki, et al. 2nd ed. Cold Spring Harbor, N.Y.: Cold Spring Harbor Laboratory Press, 2009. 1-51.

2. Varki, A., and J. B. Lowe. "Biological Roles of Glycans." *Essentials of Glycobiology*. Eds. A. Varki, et al. 2nd ed. Cold Spring Harbor, N.Y.: Cold Spring Harbor Laboratory Press, 2009. 1-22.

3. Varki, A., and T. Angata. "Siglecs - the Major Subfamily of I-Type Lectins." *Glycobiology* 16.1 (2006): 1R-27R.

4. Varki, A. C., R. Cummings, J. Esko, H. Freeze, P. Stanley, C. Bertozzi, G. Hart, and M. Etzler *Essentials of Glycobiology*. 2nd ed. Cold Spring Harbor: Cold Spring Harbor Laboratory Press, 2009.

5. Cummings, R., and J. Esko. "Principles of Glycan Recognition." *Essentials of Glycobiology*. Eds. A. Varki, et al. 2nd ed. 27 Vol. Cold Spring Harbor, N.Y.: Cold Spring Harbor Laboratory Press1-33.

6. Cummings, R., and F. T. Liu. "Chapter 33 Galectins." *Essentials of Glycobiology*. Eds. A. Varki, et al. 2nd ed. Cold Spring Harbor, N.Y.: Cold Spring Harbor Laboratory Press, 2009. 1-11.

7. Pace, K., C. Lee, P.L. Stewart, and L.G. Baum. "Restricted Receptor Segregation into Membrane Microdomains Occurs on Human T Cells During Apoptosis Induced by Galectin-1." *Journal of Immunology* 163.7 (1999): 3801-3811

8. Godula, K., and C. Bertozzi. "Density Variant Glycan Microarray for Evaluating Cross-Linking of Mucin-Like Glycoconjugates by Lectins." *Journal of the American Chemical Society* 134.38 (2012): 15732-42.

9. Kanai, M., K. Mortell, and L. Kiessling. "Varying the Size of Multivalent Ligands: The Dependence of Concanavalin A Binding on Neoglycopolymer Length." *Journal of the American Chemical Society* 119 (1997): 9931-2.

10. Dam, T., and C. F. Brewer. "Carbohydrate-Lectin Cross-Linking Interactions: Structural, Thermodynamic, and Biological Studies." *Methods in Enzymology* 362 (2003): 455-86.

11. Sacchettini, J., L. Baum, and C. F. Brewer. "Multivalent Protein-Carbohydrate Interactions. A New Paradigm for Supermolecular Assembly and Signal Transduction." *Biochemistry* 40.10 (2001): 3009-15.

12. Kuhlman, M., K. Joiner, and R.A. Ezekowitz. "The Human Mannose-Binding Protein Functions as an Opsonin." *The Journal of Experimental Medicine* 169 (1989): 1733-45.

13. Taylor, M., and K. Drickamer. *Introduction to Glycobiology*. 3rd ed. New York: Oxford University Press Inc., 2011.

14. Schuck, P., and H. Zhao. "The Role of Mass Transport Limitation and Surface Heterogeneity in the Biophysical Characterization of Macromolecular Binding Processes by SPR Biosensing." *Methods in Molecular Biology*.627 (2010): 15-54.

15. Dam., T., H.J. Gabious, S. André, H. Kaltner, M. Lensch, and F.C. Brewer. "Galectins Bind to the Multivalent Glycoprotein Asialofetuin with Enhanced Affinities and a Gradient of Decreasing Binding Constants." *Biochemistry* 44 (2005): 12564-71.

16. Schena, M. *Microarray Analysis*. Hoboken, NJ: John Wiley & Sons, Inc., 2003.

17. Schena, M., D. Shalon, R.W. Davis, and P.O. Brown "Quantitative Monitoring of Gene Expression Patterns with Complementary DNA Microarray." *Science*.270 (1995): 467-70.

18. Macbeath, G., and S. Schreiber. "Printing Proteins as Microarrays for High-Throughput Function Determination." *Science* 289.5485 (2000): 1760-3.

19. Park, S., J.C. Gildersleeve, O. Blixt, and I. Shin "Carbohydrate Microarrays." *Chemical Society Reviews* 42.10 (2013): 4310-26.

20. Wang, D., S. Liu, B.J. Trummer, C. Deng, and A. Wang "Carbohydrate Microarrays for the Recognition of Cross-Reactive Molecular Markers of Microbes and Host Cells." *Nature Biotechnology* 20.3 (2002): 275-81.

21. Galanina, O. E., M. Mecklenburg, N.E. Nifantiev, G.V. Pazynina, and N.V. Bovin. "GlycoChip: Multiarray for the Study of Carbohydrate-Binding Proteins." *Lab on a Chip* 3.4 (2003): 260-5.

22. Houseman, B., and M. Mrksich. "Carbohydrate Arrays for the Evaluation of Protein Binding and Enzymatic Modification." *Chemistry & Biology* 9 (2002): 443-454.

23. Park, S., and I. Shin. "Fabrication of Carbohydrate Chips for Studying Protein-Carbohydrate Interactions." *Angewandte Chemie International Edition* 41.17 (2002): 3180-2.

24. Houseman, B., and M. Mrksich. "Carbohydrate Arrays for the Evaluation of Protein Binding and Enzymatic Modification." *Chemistry & Biology* 9 (2002): 443-454.

25. Köhn, M., R. Wacker, C. Peters, H. Schröder, L. Soulère, R. Breinbauer, C.M. Niemeyer, and H. Waldmann. "Staudinger Ligation: A New Immobilization Strategy for the Preparation of Small-Molecule Arrays." *Angewandte Chemie International Edition* 42.47 (2003): 5830-4.

26. Disney, M., and P. Seeberger. "The use of Carbohydrate Microarrays to Study Carbohydrate-Cell Interactions and to Detect Pathogens." *Chemistry & Biology* 11.12 (2004): 1701-7.

27. Sun, X. L., C.L. Stabler, C.S. Cazalis, and E.L. Chaikof. "Carbohydrate and Protein Immobilization Onto Solid Surfaces by Sequential Diels-Alder and Azide-Alkyne Cycloadditions." *Bionconjugate Chem.* 17 (2006): 52-7.

28. Lee, M., and I. Shin. "Facile Preparation of Carbohydrate Microarrays by Site-Specific, Covalent Immobilization of Unmodified Carbohydrates on Hydrazide-Coated Glass Slides." *Organic Letters* 7.19 (2005): 4269-72.

29. Liang, P. H., S. K. Wang, and C. H. Wong. "Quantitative Analysis of Carbohydrate-Protein Interactions using Glycan Microarrays: Determination of SUrface and Solution Dissociation Constants." *Journal of the American Chemical Society* 129.36 (2007): 11177-84.

30. He, X., and D. Carter. "Atomic Structure and Chemistry of Human Serum Albumin." *Nature* 358.6383 (1992): 209-15

31. Oyelaran, O., Q. Li, D. Farnsworth, J.C. Gildersleeve "Microarrays with Varying Carboyhydrate Density Reveal Distinct Subpopulations of Serum Antibodies." *Journal of Proteome Research* 8 (2009): 3529-38.

32. Godula, K., D. Rabuka, K.T. Nam, and C. Bertozzi "Synthesis and Microcontact Printing of Dual End-Functionalized Mucin-Like Glycopolymers for Microarray Applications." *Angewandte Chemie International Edition* 48.27 (2009): 4973-6

33. Godula, K., C. Bertozzi. “Density variant glycan microarray for evaluating cross-linking of mucin-like glycoconjugates by lectins.” *Journal of the American Chemical Society* 134.38 (2012): 15732-42

34. Heimburg-Molinaro, J., X. Song, D.F. Smith, R.D. Cummings "Preparation and Analysis of Glycan Microarrays." *Current Protocols in Protein Science* 64.12.10 (2011): 1-29.

35. Huang, M., R.A.A. Smith, G.W. Trieger, and K. Godula "Glycocalyx Remodeling with Proteoglycan Mimetics Promotes Neural Specification in Embryonic Stem Cells." *Journal of the American Chemical Society* 136.30 (2014): 10565-8.

36. Groll, J., Z. Ademovic, T. Ameringer, D. Klee, M. Moeller "Comparison of Coatings from Reactive Star Shaped PEG-Stat-PPG Prepolymers and Grafted Linear PEG for Biological and Medical Applications." *Biomacromolecules* 6.2 (2005): 956-62

37. Kingshott, P., H. Thissen, and H. Griesser. "Effects of Cloud-Point Grafting, Chain Length, and Density of PEG Layers on Competitive Adsorption of Ocular Proteins." *Biomaterials* 23.9 (2002): 2043-56.

38. Nakajima, N., and Y. Ikada. "Mechanism of Amide Formation by Carbodiimide for Bioconjugation in Aqueous Media." *Bioconjugate Chem.* 6.1 (1995): 123-30.

39. Zhu, X. and Y. Deng. "Transport at the Air/Water Interface is the Reason for Rings in Protein Microarrays." *Journal of the American Chemical Society Communications*. 128 (2006): 2768-69.

40. Chan, T., R. Hilgraf, K.B. Sharpless, and V.V. Fokin. "Polytriazoles as Copper(I)-Stabilizing Ligands in Catalysis." *Organic Letters* 6.17 (2004): 2853-5.

41. Macbeath, G., and S. Schreiber. "Printing Proteins as Microarrays for High-Throughput Function Determination." *Science* 289.5485 (2000): 1760-3.

42. Matson, R. "Microarray Methods and Protocols." *CRC Press*, 2009.

43. Ghaemi, S., F. Harding, B. Delalat, R. Vasani, N. Voelcker "Surface Engineering for Long-Term Culturing of Mesenchymal Stem Cell Microarrays." *Biomacromolecules* 14.8 (2013): 2675-83.

44. Matson, R., R. Milton, R. Obremski, J.W. Silzel Multi-Functional Microarrays and Methods. Patent WO2003091446 A2. Nov 6, 2003.

45. Grace Bio-Labs. "ONCYTE Guide to Protein Microarrays." *Grace Bio-Labs* (2011).

46. Sharma, V., M. Vijayan, A. Surolia. "Imparting Exquisite Specificity to Peanut Agglutinin for the Tumor-associated Thomson-Friedenreich Antigen by Redesign of Its Combining Site." *Journal of Biological Chemistry* 271 (1996) 21209-21213.

47. Paz, J. and P. Seeberger. *Carbohydrate Microarrays.* Ed. Y. Chevelot. Vol 808. Humana Press, 2012. Recent Advantages and Future Challenge in Glycan Microarray Technology.

48. Attie, A. and R. Raines. "Analysis of Receptor-Ligand Interactions." *Journal of Chemical Education* 72.2 (1995) 119-124.

49. Liang, P., S. Wang, C. Wong. “Quantitative Analysis of Carbohydrate-Protein Interactions Using Glycan Microarrays: Determination of Surface and Solution Dissociation Constants.” *Journal of the American Chemical Society* 129.36 (2007) 11177-84.

50. Cummings, R. and M. E. Etzler “Chapter 28, R-type Lectins.” *Essentials of Glycobiology*. Eds. A. Varki, et. al. 2nd ed. Cold Spring Harbor, N.Y.: Cold Spring Harbor Laboratory Press, 2009, 1-11.

Appendix

Carboxylic Acid Polymer, 195 Lactose, n=273

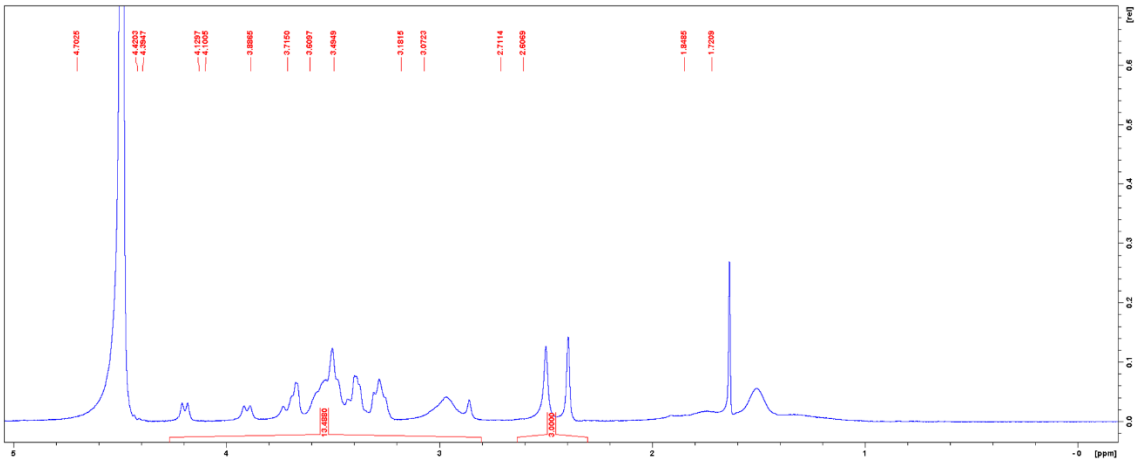

Carboxylic Acid Polymer, 59 Lactose, n=273

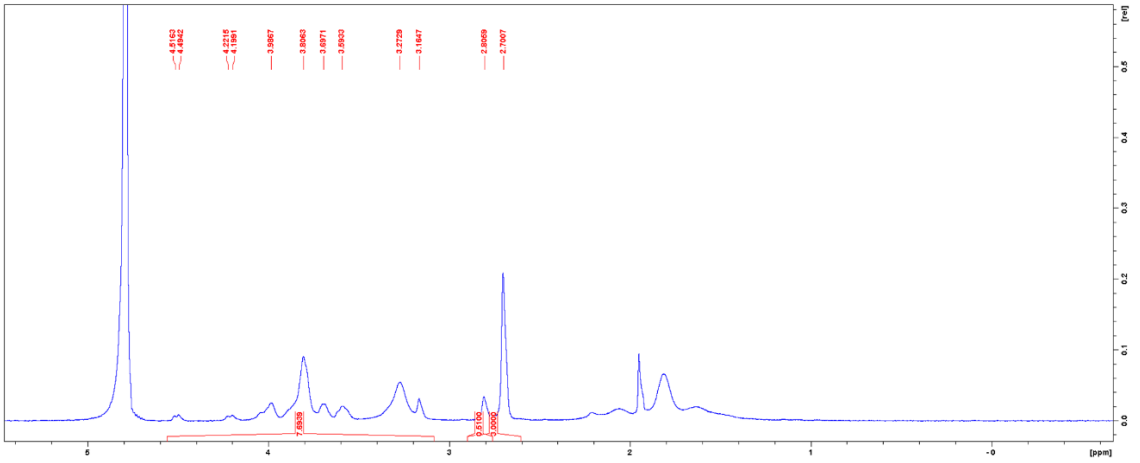

Carboxylic Acid Polymer, 179 LacNAc, n=273

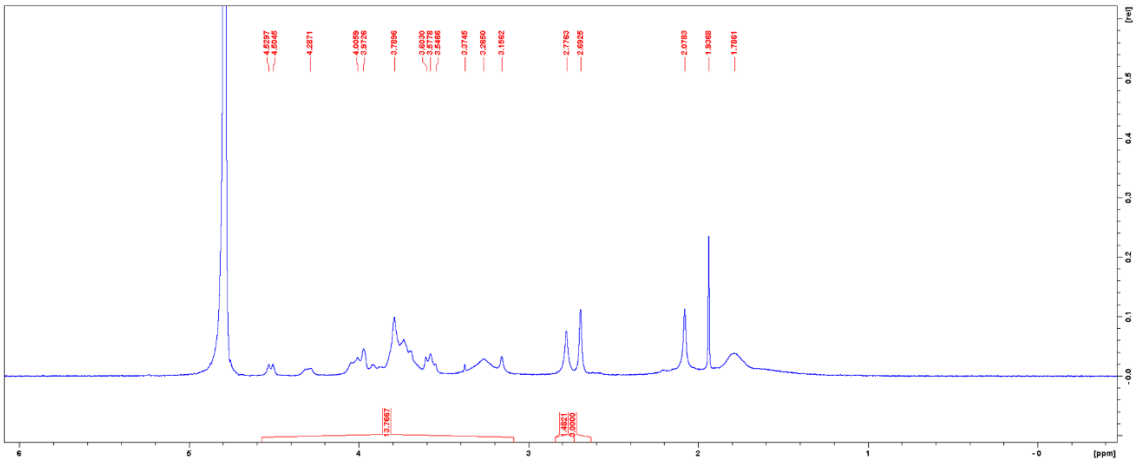

Carboxylic Acid Polymer, 88 LacNAc, n=273

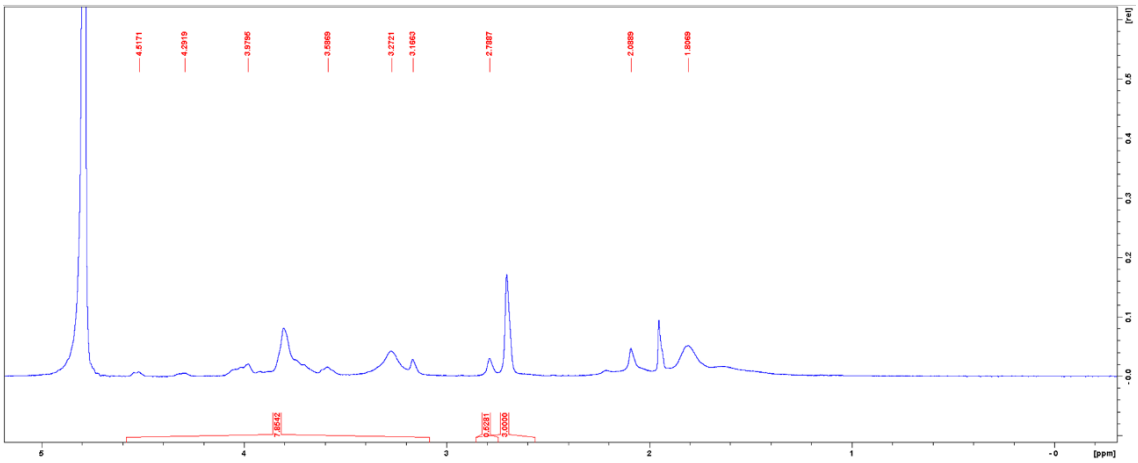

Azide Polymer, 110 Lactose, n=150

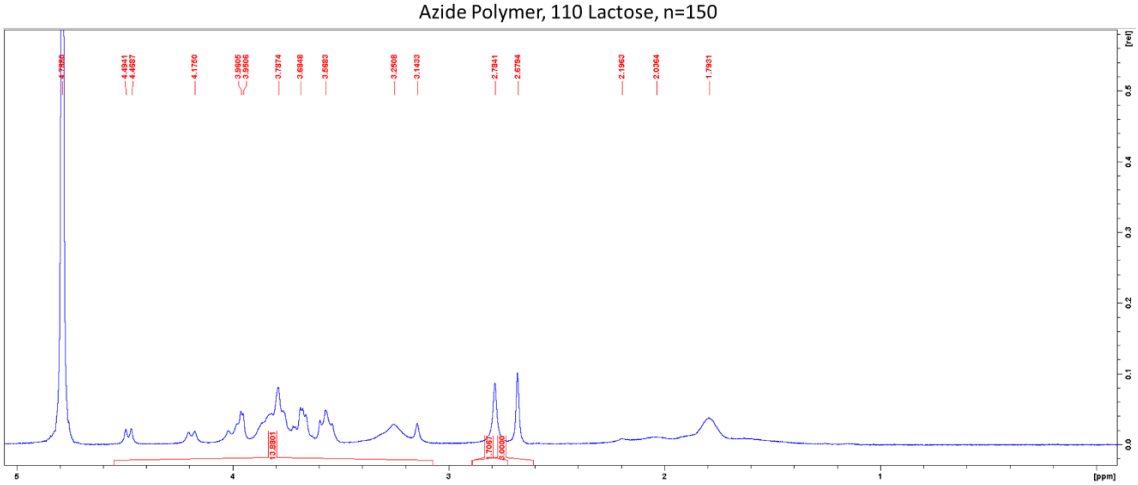

Azide Polymer, 78 Lactose, n=150

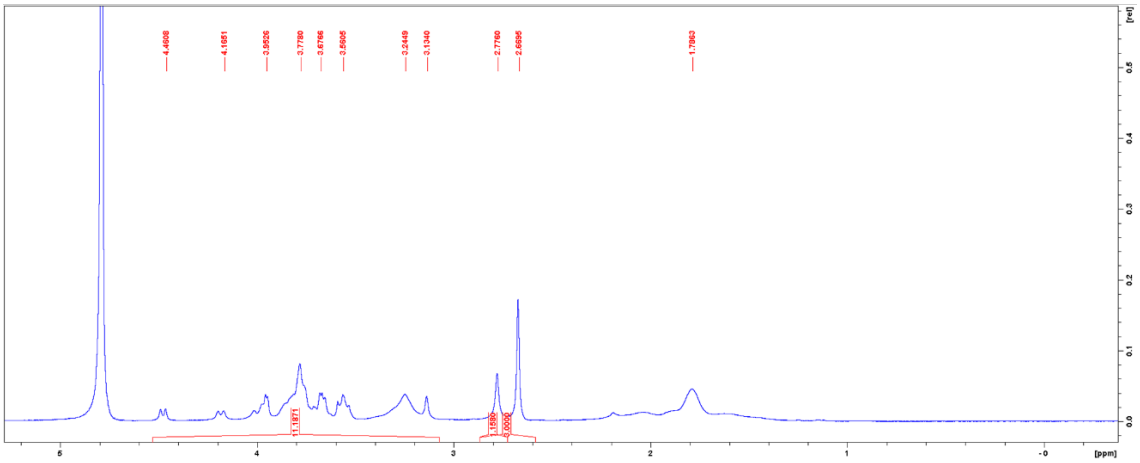

Azide Polymer, 45 Lactose, n=150

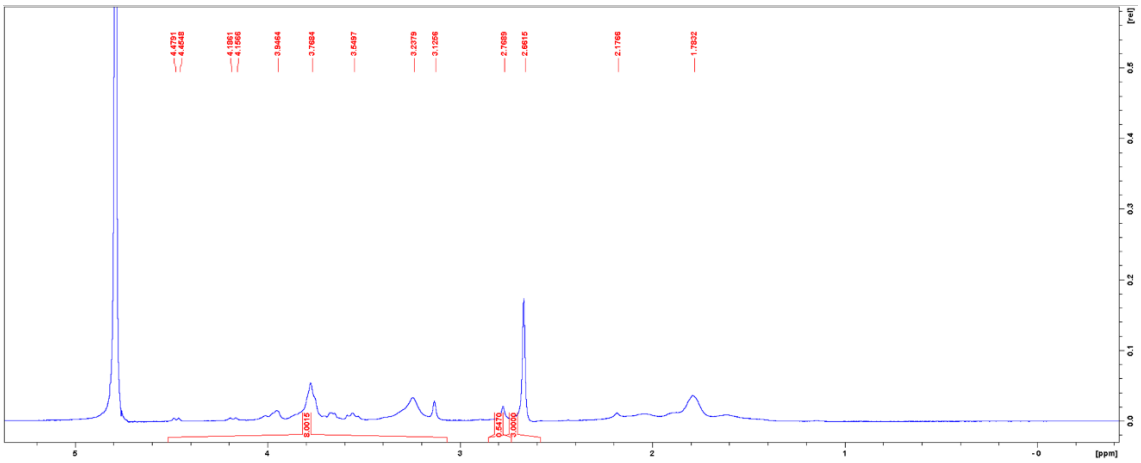

Azide Polymer, 96 LacNAc, n=150

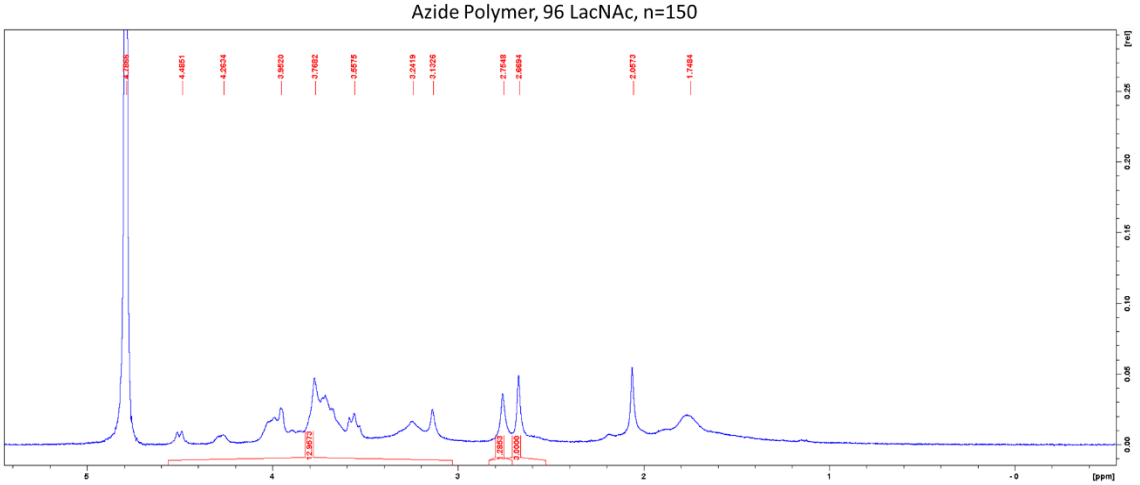

Azide n=150 Polymer, 54 LacNAc

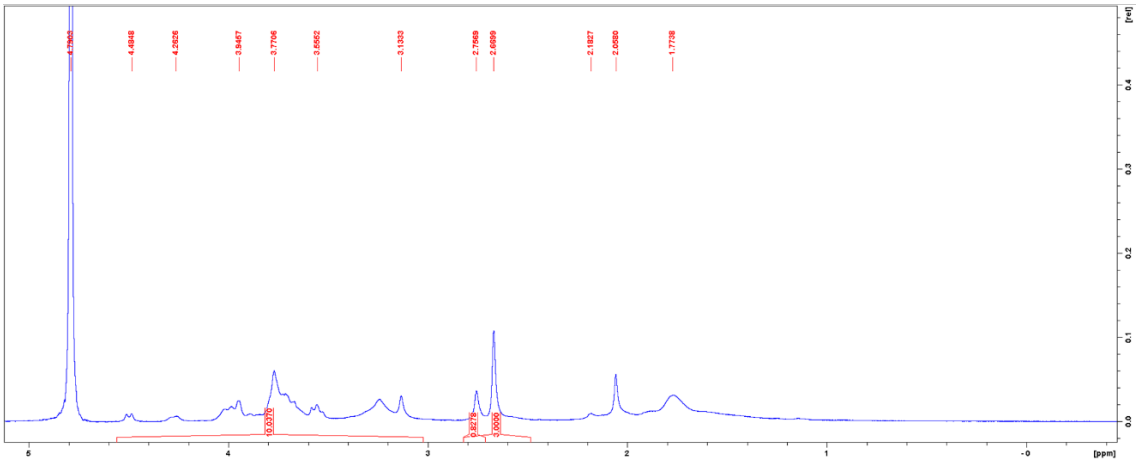

Azide Polymer, 24 LacNAc, n=150

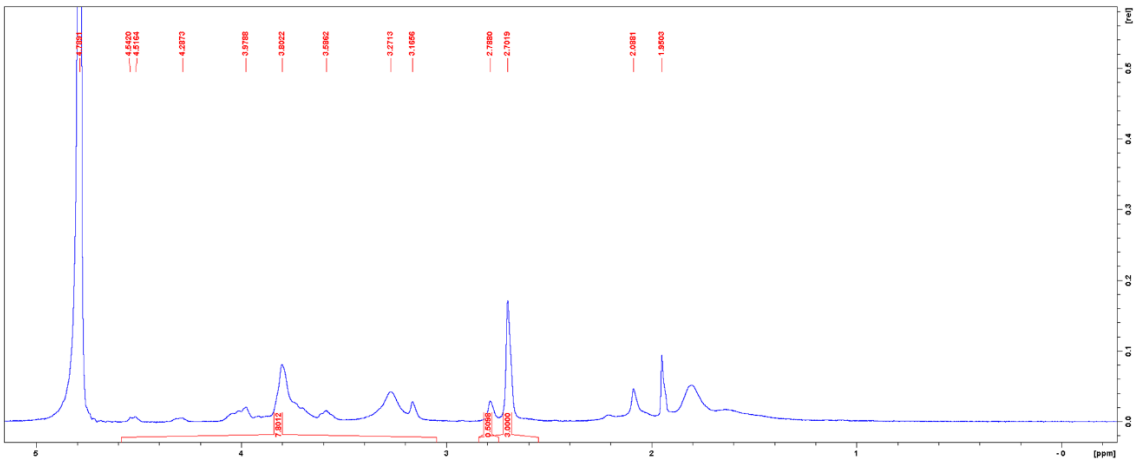

Azide Polymer, 134 Cellobiose, n=150

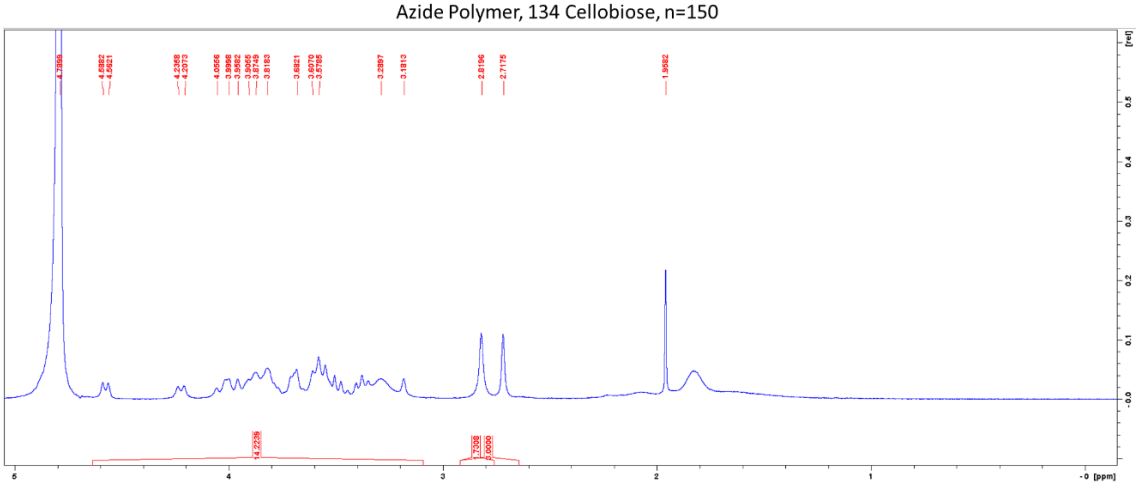

Azide Polymer, 129 Glucose, n=150

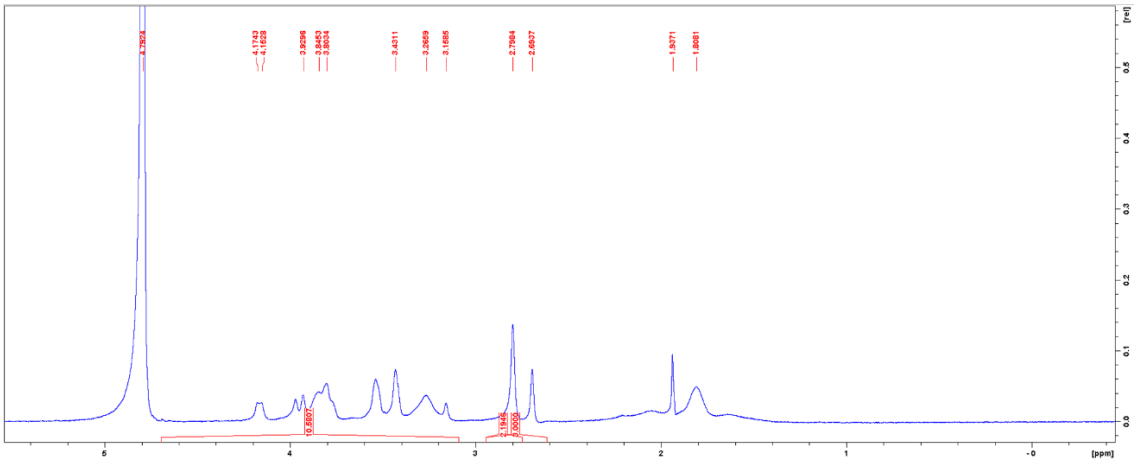

Azide Polymer, 253 Lactose, n=424

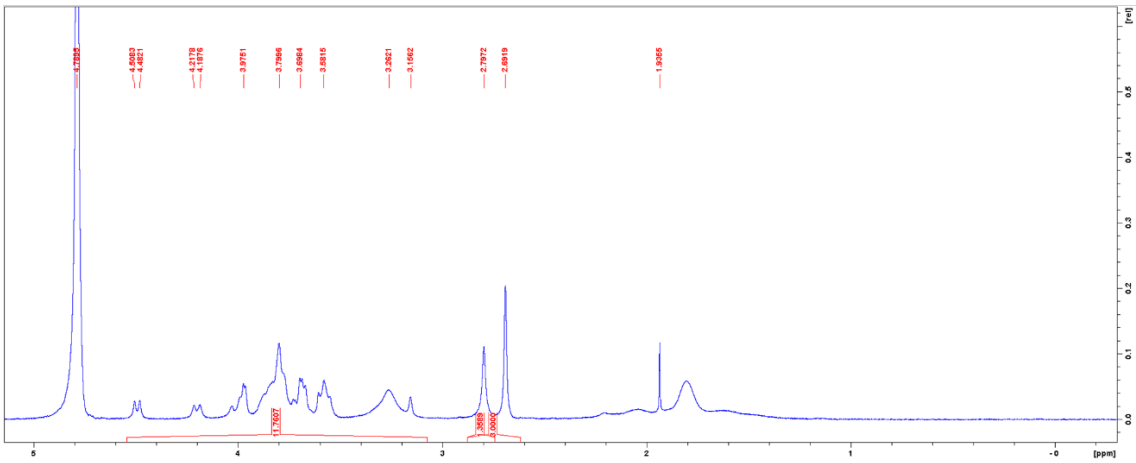

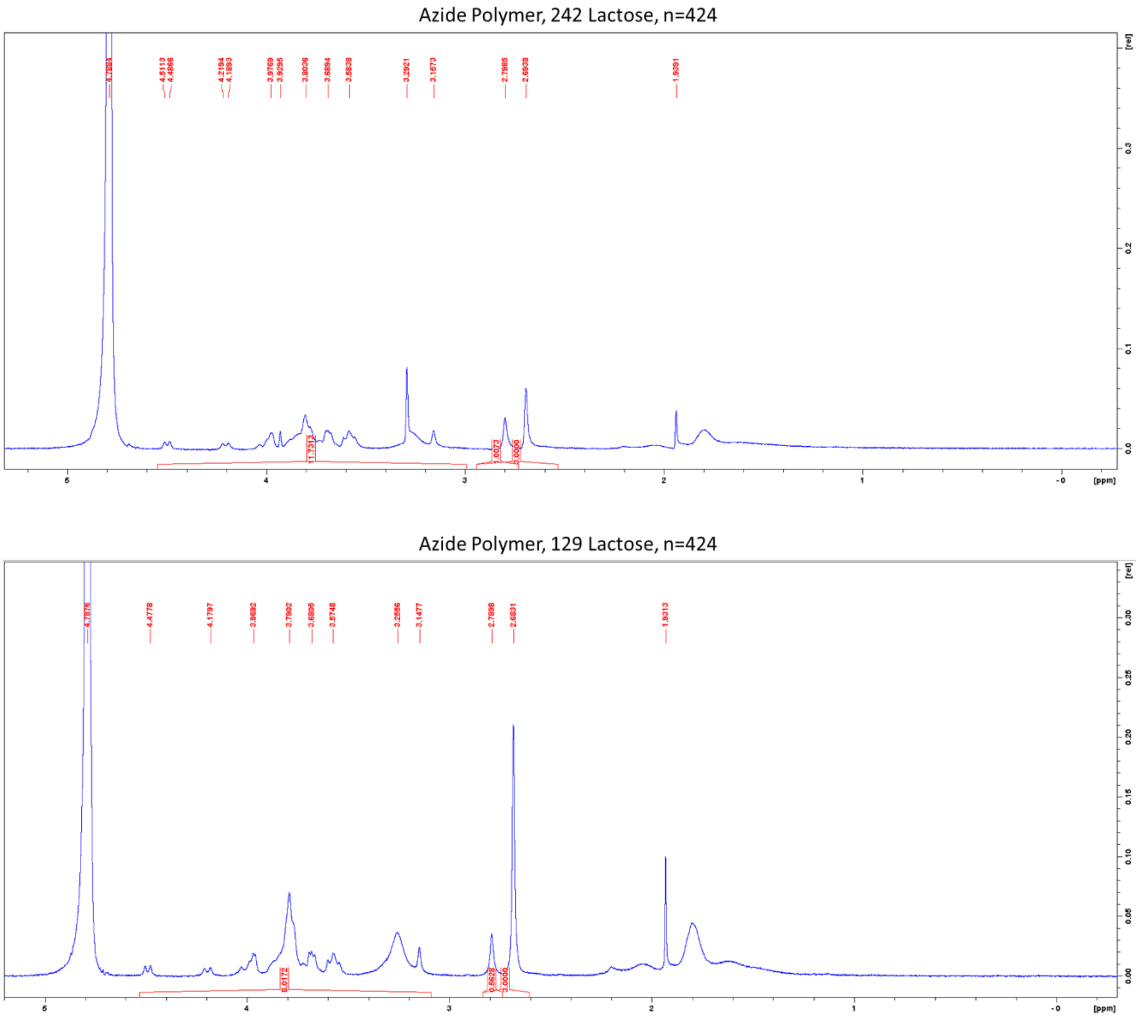

Figure 6.1: ^{1}H NMR of the various polymers used.

Table 6.1: Glycopolymer characteristics

Polymer Length	Glycan	Glycan Equivalent Used	Ligation Efficiency, %	Valency
150	Lactose	1.1 eq	73%	110
150	Lactose	0.6 eq	52%	78
150	Lactose	0.2 eq	30%	45
150	LacNAc	1.1 eq	64%	96
150	LacNAc	0.6 eq	36%	54
150	LacNAc	0.2 eq	16%	24
150	Cellobiose	1.1 eq	89%	134
150	Glucose	1.1 eq	86%	129
212	Lactose	1.1 eq	65%	139
212	Lactose	0.8 eq	57%	120
212	Lactose	0.6 eq	49%	103
212	Lactose	0.4 eq	33%	71
212	Lactose	0.2 eq	28%	59
212	LacNAc	1.1 eq	78%	165
212	LacNAc	0.8 eq	47%	100
212	LacNAc	0.6 eq	45%	95
212	LacNAc	0.4 eq	32%	68
212	LacNAc	0.2 eq	17%	36

Table 6.1: Glycopolymer characteristics, continued.

Polymer Length	Glycan	Glycan Equivalent Used	Ligation Efficiency, %	Valency
212	Lactose	1.1 eq	73%	110
212	Lactose	0.6 eq	52%	78
273 -COOH	Lactose	0.2 eq	30%	45
273 -COOH	LacNAc	1.1 eq	64%	96
273 -COOH	LacNAc	0.6 eq	36%	54
273 -COOH	LacNAc	0.2 eq	16%	24
273 -COOH	Cellobiose	1.1 eq	89%	134
273 -COOH	Glucose	1.1 eq	86%	129
424	Lactose	1.1 eq	65%	139
424	Lactose	0.8 eq	57%	120
424	Lactose	0.6 eq	49%	103

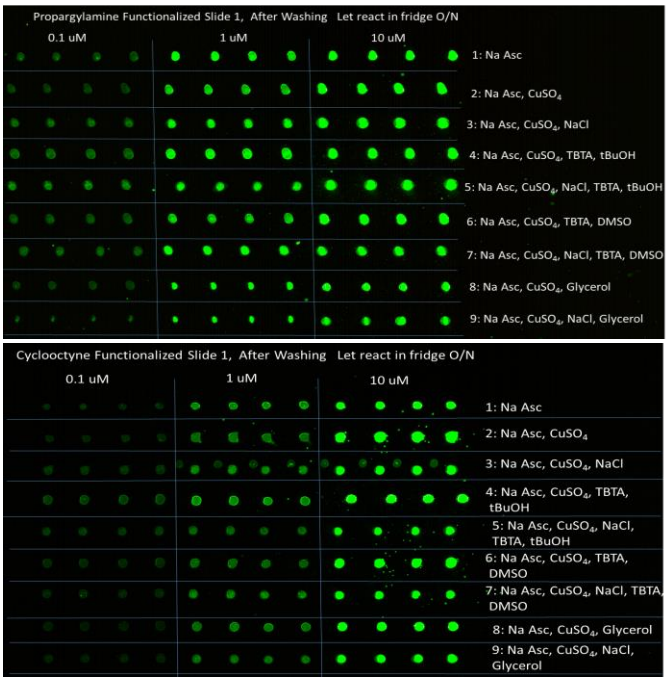

Figure 6.2: Propargylamine vs Cyclooctyne Functionalization Print

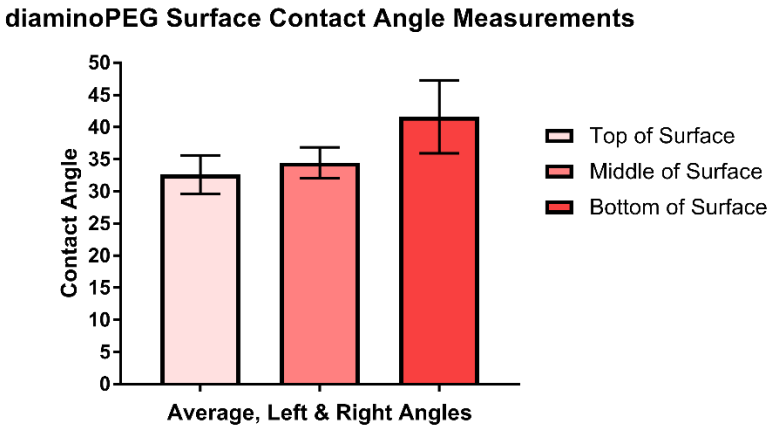

Figure 6.3: Characterization of diaminoPEG Substrate Surfaces using Contact Angle Measurements throughout the Substrate Surface.

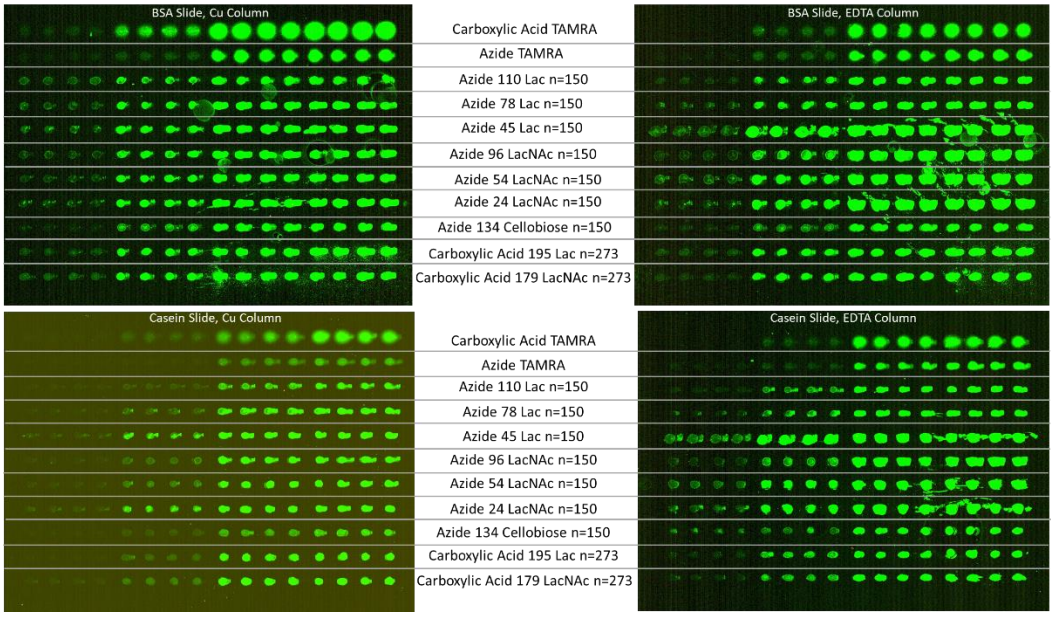

Figure 6.4: Images of the BSA and Casein Passivation test. diaminoPEG-propargyl slides were passivated in either 1% BSA or 1 % Casein for 1 hour prior to printing. The left column of the slide was printed in a printing buffer containing copper, whereas the right column was printed in a buffer containing EDTA using a separate pin.

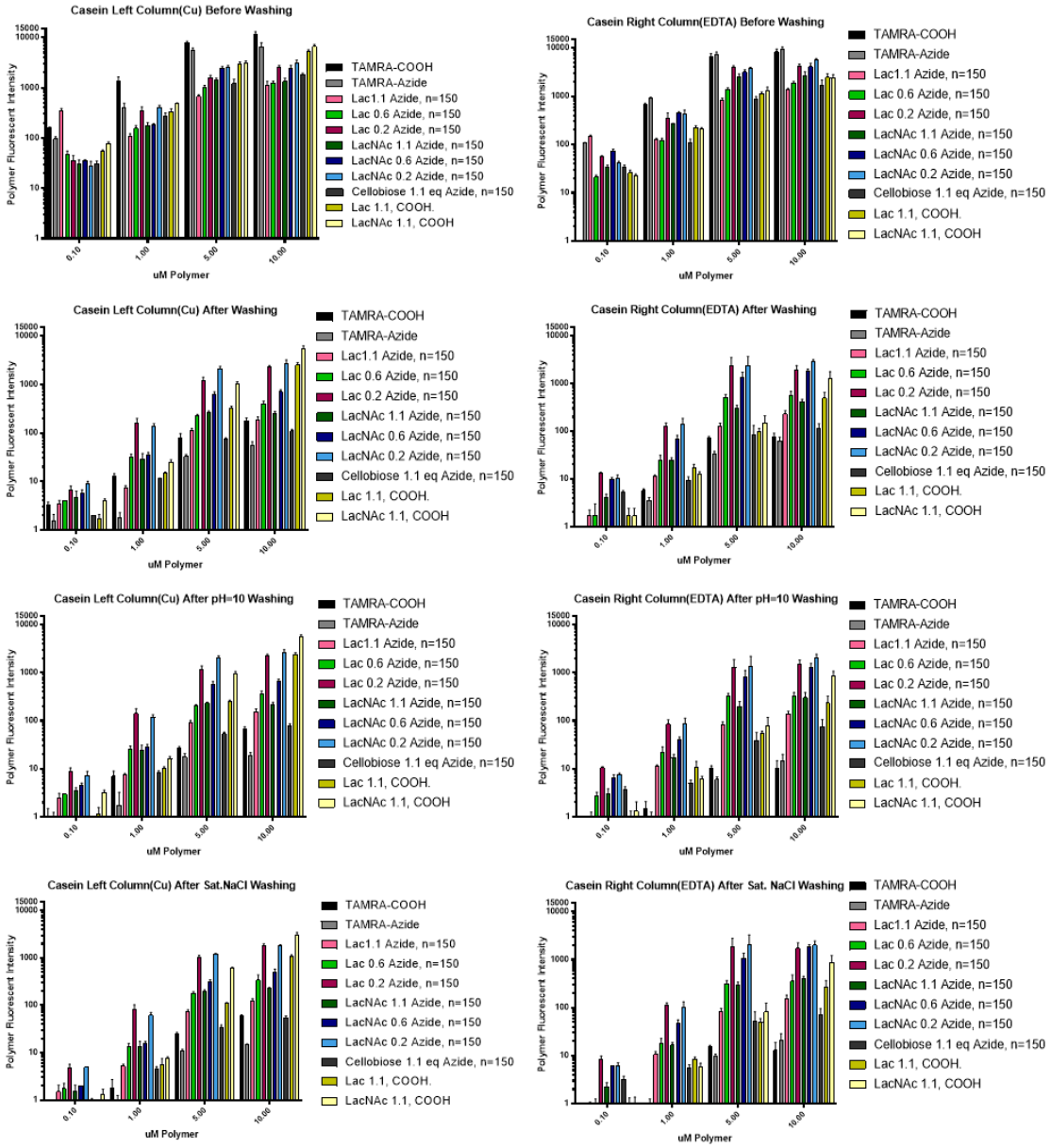

Figure 6.5: Effect of Multiple Washes on Polymer Printed onto Casein and BSA Passivated Slides.

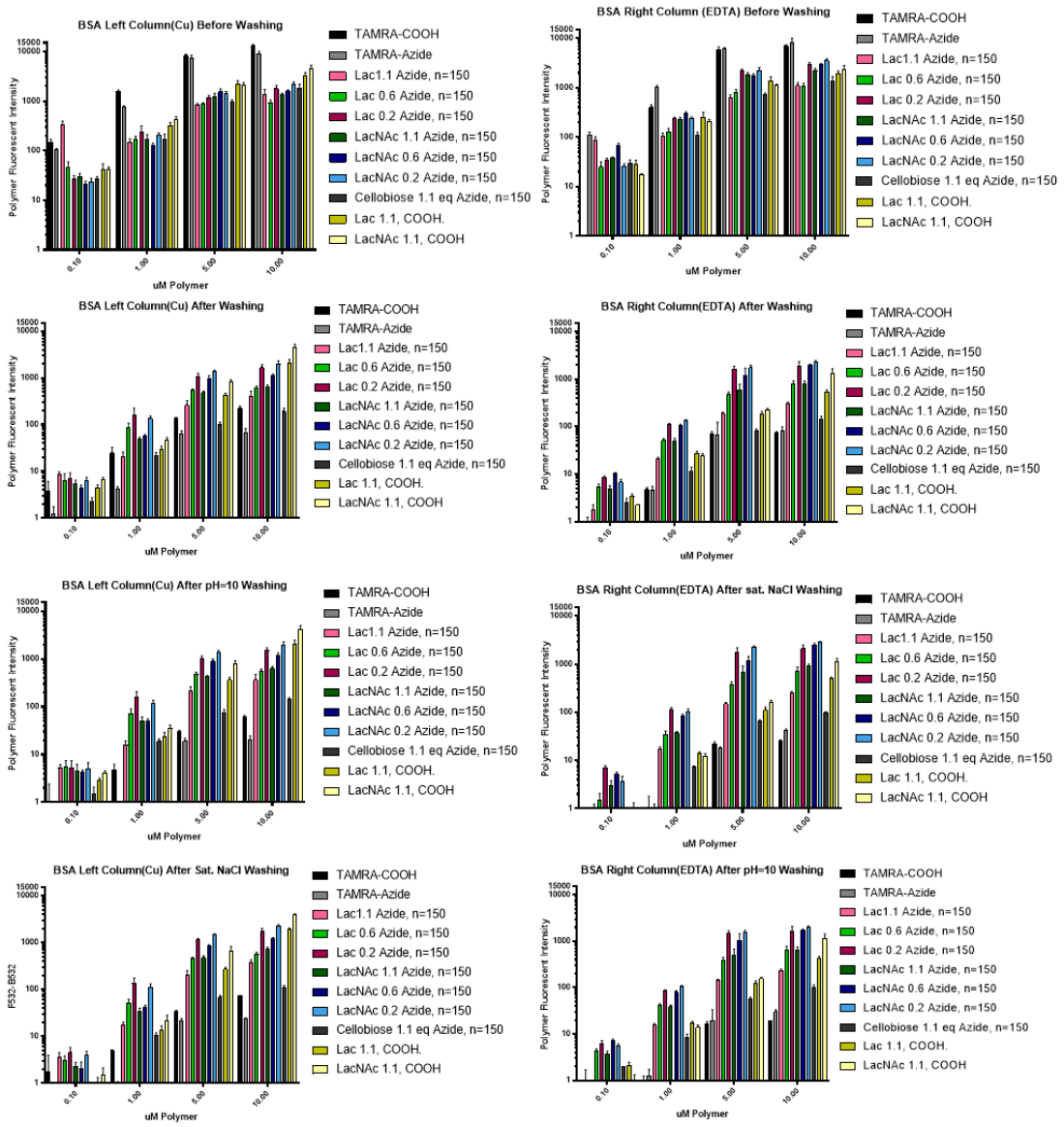

Figure 6.5: Effect of Multiple Washes on Polymer Printed onto Casein and BSA Passivated Slides Continued.

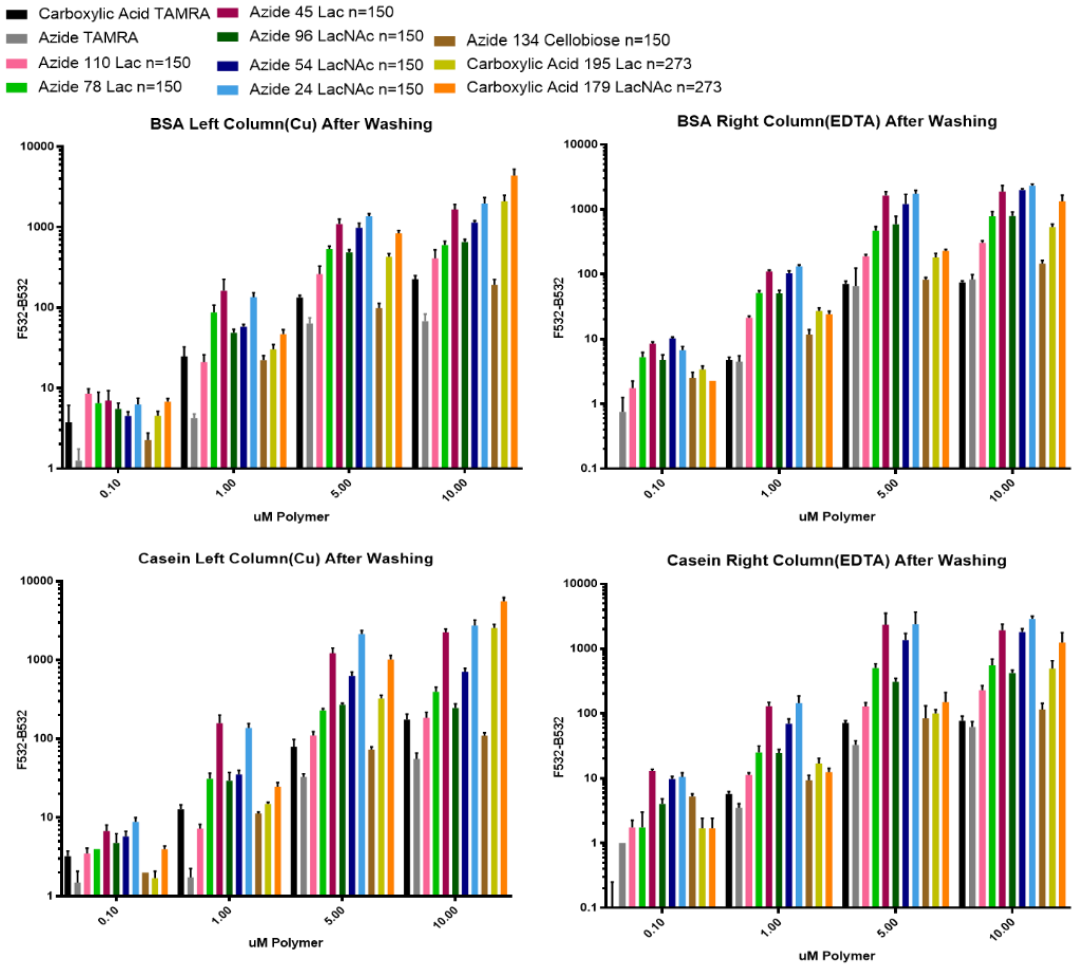

Figure 6.6: Evaluation of fluorescence lost on a commercially obtained high-density alkyne slide, all conditions tested.

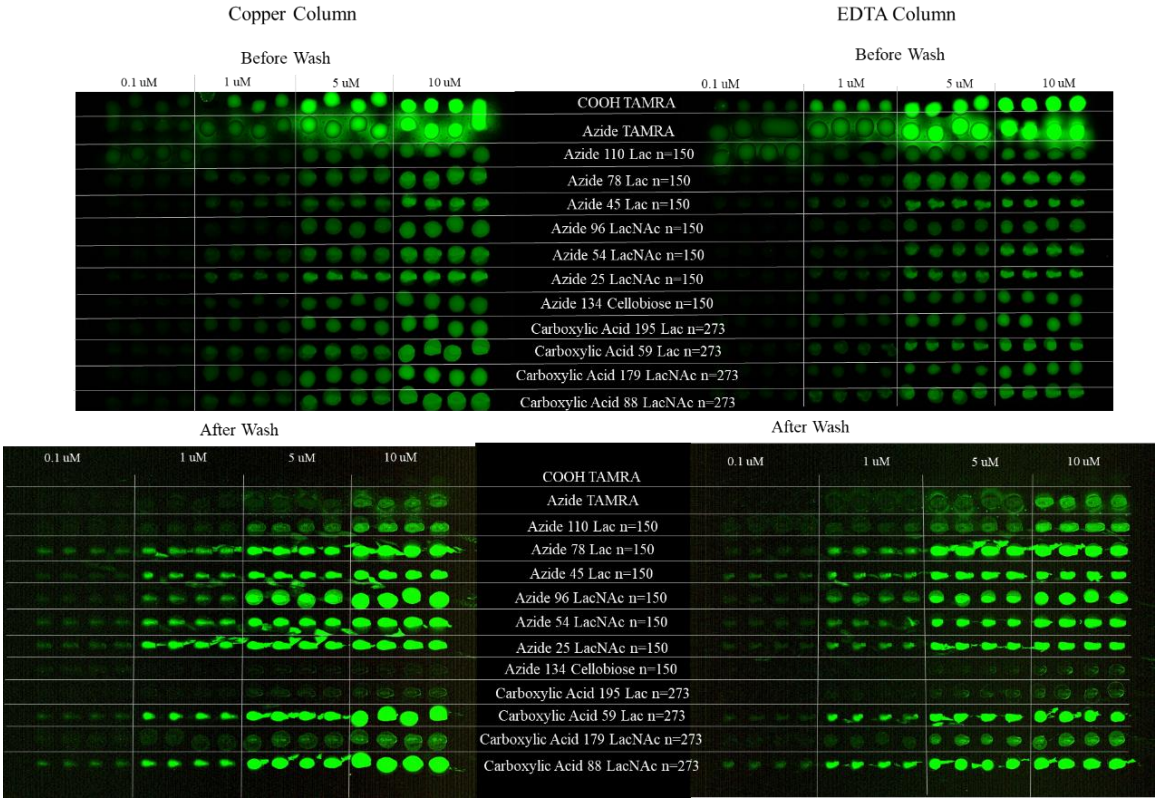

Figure 6.7 Images of the commercially obtained high-density alkyne slide, before and after washing.

Replicate 1, Right Column:

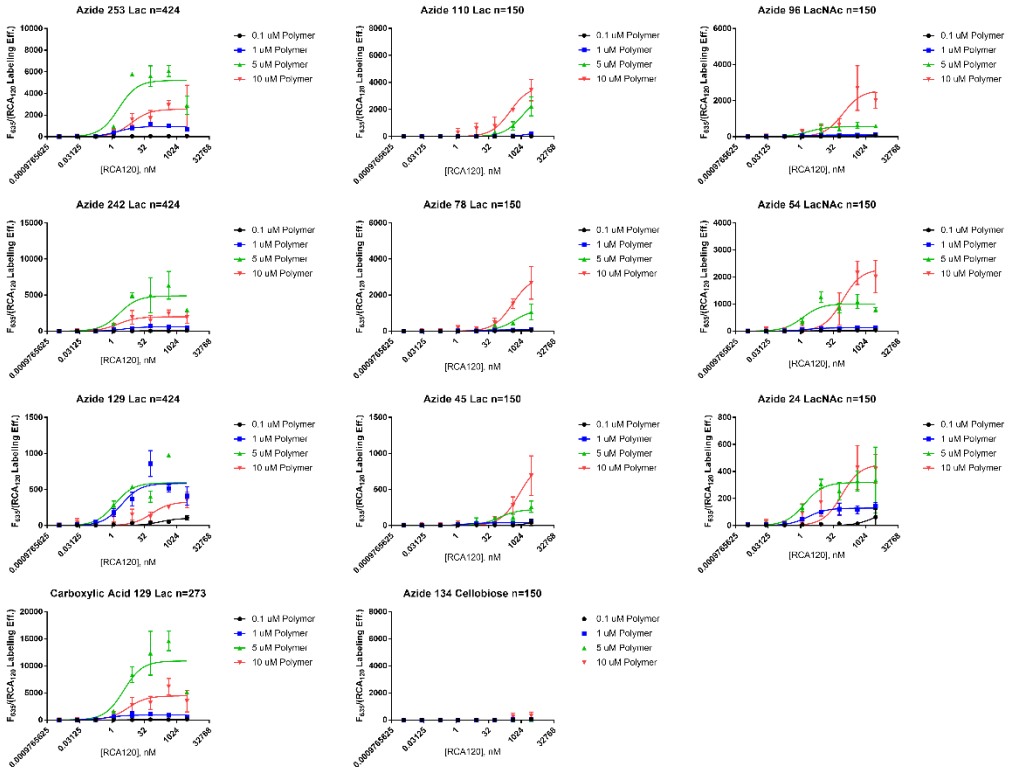

Azide 253 Lac, n=424

[Glycopolymer]	Apparent K_D	Std. Error	R^2
10 µM	8.051	5.175	0.7026
5 µM	2.036	0.9303	0.7925
1 µM	1.805	0.5476	0.8885
0.1 µM	4.056	1.552	0.8106

Azide 110 Lac n=150

[Glycopolymer]	Apparent K_D	Std. Error	R^2
10 µM	314.2	102.2	0.8796
5 µM	1155	402	0.8952
1 µM	3742	4070	0.772
0.1 µM	831.4	1143	0.2096

Azide 96 LacNAc n=150

[Glycopolymer]	Apparent K_D	Std. Error	R^2
10 µM	92.34	44.53	0.7472
5 µM	2.265	0.9685	0.7997
1 µM	1.23	0.4087	0.8489
0.1 µM	1721	1546	0.5735

Azide 242 Lac, n=424

[Glycopolymer]	Apparent K_D	Std. Error	R^2
10 µM	1.992	1.088	0.7173
5 µM	2.171	1.185	0.73
1 µM	3.778	1.167	0.8861
0.1 µM	9.364	5.306	0.6479

Azide 78 Lac n=150

[Glycopolymer]	Apparent K_D	Std. Error	R^2
10 µM	*401.5*	*106.5*	*0.9023*
5 µM	501.8	195	0.8122
1 µM	20.02	13.55	0.5669
0.1 µM	153.5	86.38	0.6195

Azide 54 LacNAc n=150

[Glycopolymer]	Apparent K_D	Std. Error	R^2
10 µM	88.22	29.59	0.8686
5 µM	1.255	0.509	0.8144
1 µM	*1.673*	*0.3852*	*0.9231*
0.1 µM	6.137	3.646	0.5948

Azide 129 Lac, n=424

[Glycopolymer]	Apparent K_D	Std. Error	R^2
10 µM	68.64	40.23	0.5169
5 µM	1.366	0.691	0.7372
1 µM	2.808	1.45	0.7353
0.1 µM	173.7	86.37	0.6775

Azide 45 Lac, n=150

[Glycopolymer]	Apparent K_D	Std. Error	R^2
10 µM	837.7	362.8	0.8431
5 µM	99.74	48.79	0.7005
1 µM	2.373	1.021	0.7471
0.1 µM	24522	294440	0.4039

Azide 24 LacNAc n=150

[Glycopolymer]	Apparent K_D	Std. Error	R^2
10 µM	80.77	38.87	0.6986
5 µM	1.498	0.7861	0.7113
1 µM	2.169	0.6891	0.8686
0.1 µM	2561	4050	0.4271

Carboxylic Acid 195 Lac n=273

[Glycopolymer]	Apparent K_D	Std. Error	R^2
10 µM	5.584	3.187	0.7326
5 µM	3.514	1.939	0.7301
1 µM	0.6569	0.3668	0.6962
0.1 µM	9.357	10.15	0.3369

Figure 6.8: Replicate binding assays of RCA$_{120}$

Replicate 2, Left Column:

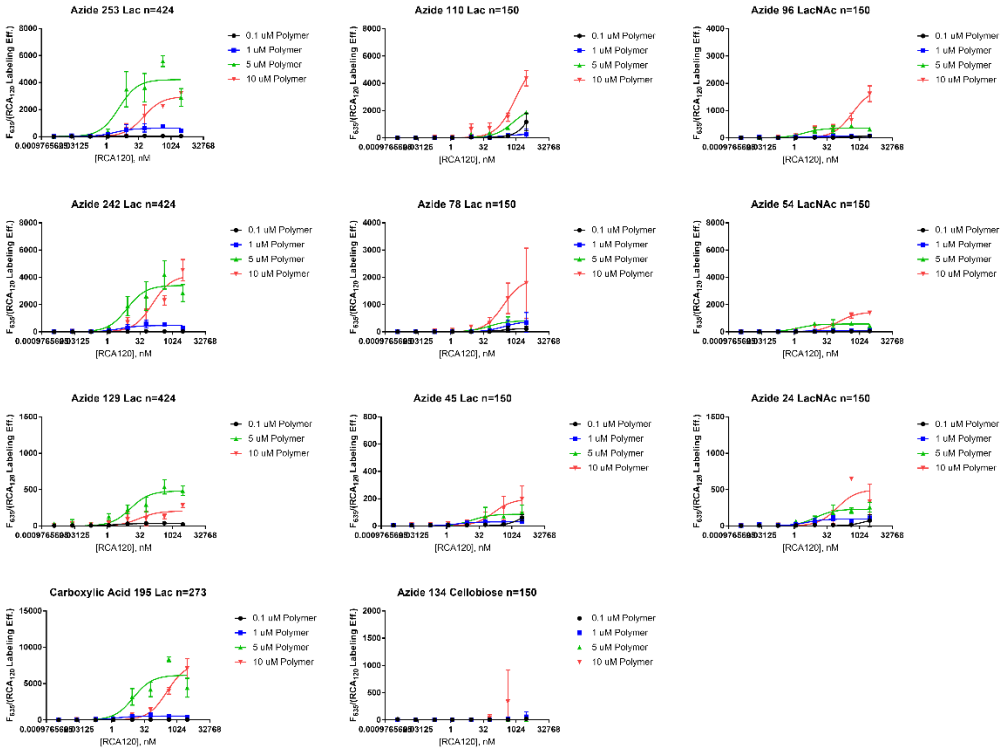

Azide 253 Lac, n=424

[Glycopolymer]	Apparent K_D	Std. Error	R^2
10 μM	55.45	14.95	0.893
5 μM	3.882	1.773	0.798
1 μM	2.513	1.452	0.675
0.1 μM	2.98	2.563	0.411

Azide 110 Lac n=150

[Glycopolymer]	Apparent K_D	Std. Error	R^2
10 μM	*937.7*	*298*	*0.9258*
5 μM	*767.4*	*154.4*	*0.9483*
1 μM	270.5	367	0.2515
0.1 μM	~ 1.538e+017	5.392E+30	0.7751

Azide 96 LacNAc n=150

[Glycopolymer]	Apparent K_D	Std. Error	R^2
10 μM	471.1	169	0.8393
5 μM	2.993	1.169	0.832
1 μM	2.069	0.9664	0.6362
0.1 μM	246.4	77.04	0.8446

Azide 242 Lac, n=424

[Glycopolymer]	Apparent K_D	Std. Error	R^2
10 μM	123.8	39.98	0.849
5 μM	8.169	3.223	0.828
1 μM	3.868	2.694	0.589
0.1 μM	4.2	3.925	0.374

Azide 78 Lac n=150

[Glycopolymer]	Apparent K_D	Std. Error	R^2
10 μM	265.8	122.8	0.7681
5 μM	55.18	17.99	0.8604
1 μM	278.6	240.6	0.4945
0.1 μM	239.1	213.6	0.4721

Azide 54 LacNAc n=150

[Glycopolymer]	Apparent K_D	Std. Error	R^2
10 μM	107.7	28.72	0.8839
5 μM	1.585	0.6982	0.788
1 μM	2.081	0.8517	0.7534
0.1 μM	55.24	34.88	0.551

Azide 129 Lac, n=424

[Glycopolymer]	Apparent K_D	Std. Error	R^2
10 μM	29.85	22.04	0.462
5 μM	11.8	4.018	0.837
1 μM	-40.15	5.516	0.556
0.1 μM	1.931	1.409	0.508

Azide 45 Lac, n=150

[Glycopolymer]	Apparent K_D	Std. Error	R^2
10 μM	148.2	65.22	0.7332
5 μM	15.22	9.942	0.5913
1 μM	2.989	1.649	0.6276
0.1 μM	7724	12042	0.8018

Azide 24 LacNAc n=150

[Glycopolymer]	Apparent K_D	Std. Error	R^2
10 μM	95.52	47.34	0.7089
5 μM	9.586	3.955	0.783
1 μM	3.595	1.881	0.6893
0.1 μM	2621	4626	0.3917

Carboxylic Acid 195 Lac n=273

[Glycopolymer]	Apparent K_D	Std. Error	R^2
10 μM	*352.9*	*69.63*	*0.965*
5 μM	10.04	4.203	0.8126
1 μM	1.598	0.9337	0.6421
0.1 μM	1.444	1.24	0.4235

Figure 6.8: Replicate binding assays of RCA_{120}, continued.

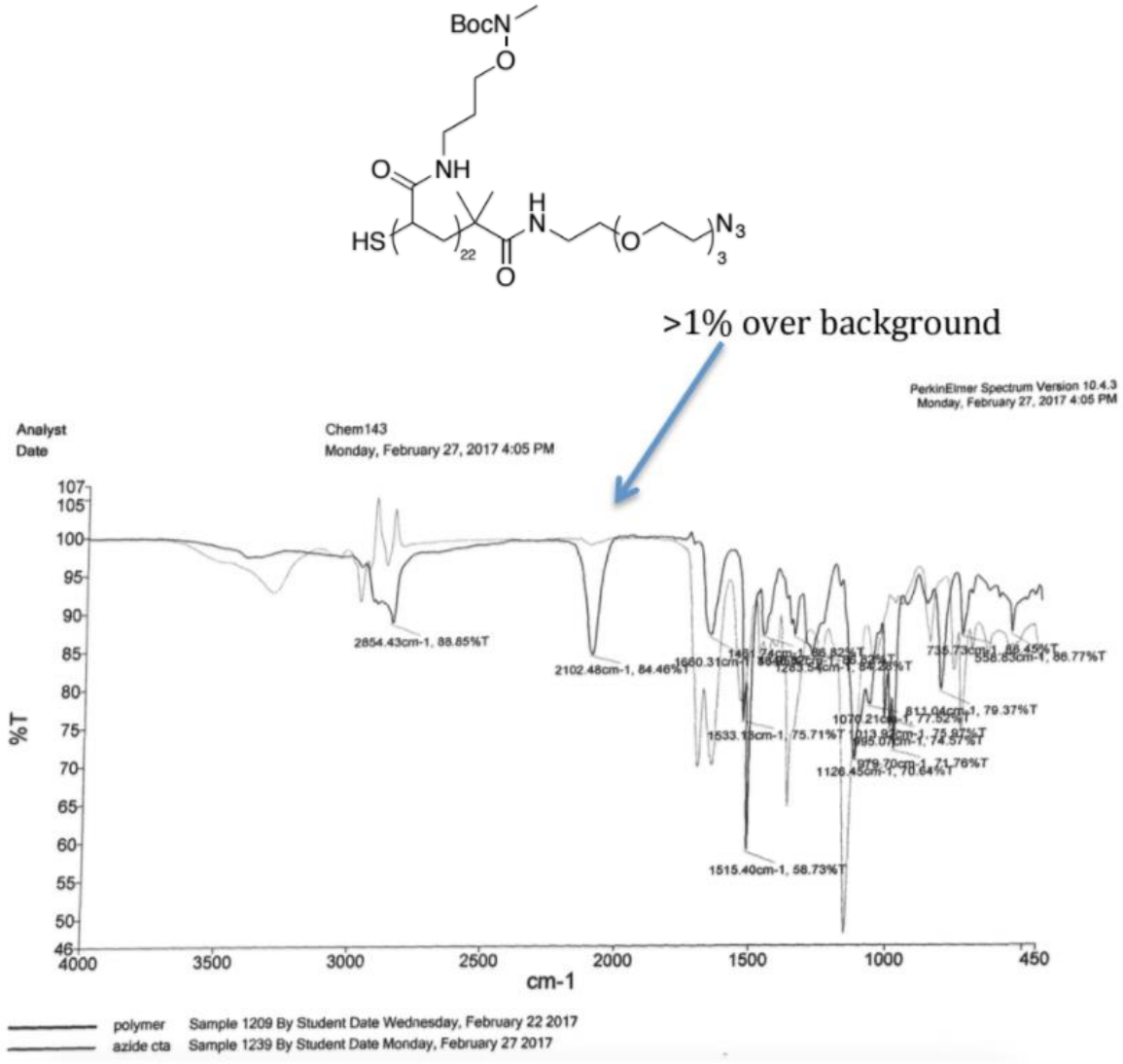

Figure 6.9: IR Data of an Azide terminated n=22 polymer. Shown in light gray is the polymer, with azide-CTA shown in dark gray.